

NACA RM E57118

CONFIDENTIAL

Langley
Copy 21
RM E57118

UNCLASSIFIED

CLASSIFICATION CHANGED

NACA

UNAVAILABLE

By authority of TPA #53 Date 7/11/61
114-209

RESEARCH MEMORANDUM

EXPERIMENTAL INVESTIGATION OF SEVERAL AFTERBURNER
CONFIGURATIONS ON A J79 TURBOJET ENGINE

By Harry E. Bloomer and Carl E. Campbell

Lewis Flight Propulsion Laboratory
Cleveland, Ohio

LIBRARY COPY
DEC 2 1957
LANGLEY AERONAUTICAL LABORATORY
LIBRARY, NACA
LANGLEY FIELD, VIRGINIA

SPECIAL RELEASE

Transmitted on _____
not to be indexed, referenced, or
given further distribution without
approval of NACA.

FOR REFERENCE

NOT TO BE TAKEN FROM THIS ROOM

CAT. NO. 1835

LIBRARY BUREAU

CLASSIFIED DOCUMENT

This material contains information affecting the National Defense of the United States within the meaning of the espionage laws, Title 18, U.S.C., Secs. 793 and 794, the transmission or revelation of which in any manner to unauthorized persons is prohibited by law.

**NATIONAL ADVISORY COMMITTEE
FOR AERONAUTICS
WASHINGTON**

CONFIDENTIAL

CONFIDENTIAL



NATIONAL ADVISORY COMMITTEE FOR AERONAUTICS

RESEARCH MEMORANDUM

EXPERIMENTAL INVESTIGATION OF SEVERAL AFTERBURNER

CONFIGURATIONS ON A J79 TURBOJET ENGINE

By Harry E. Bloomer and Carl E. Campbell

SUMMARY

4644
CI-1

An investigation was conducted in an NACA altitude test chamber to evaluate several afterburner configurations on an XJ79 engine. Data were obtained from nine configurations which show the effect on burner performance of increased burner diameter and modifications to the flameholder, fuel system, and flow swirl. The data for the configurations were obtained for a range of afterburner-inlet total pressures from 860 to 3290 pounds per square foot absolute at a burner-inlet temperature of 1530° R.

Simple fuel system and flameholder modifications to the original prototype configuration increased the combustion efficiency and lowered the pressure drop resulting in substantial thrust increases. Applying these modifications to a larger diameter burner resulted in further performance gains at all flight conditions investigated. At 59,400 feet and a Mach number of 2.0, the thrust advantages for the large burner over the small burner amounted to 19 percent, and the specific fuel consumption was lower by approximately 10 percent.

INTRODUCTION

During an investigation of the altitude performance and operational characteristics of an XJ79 engine in an NACA altitude test chamber, the afterburner performance was evaluated. In the preliminary stage of this evaluation, the performance was below that required to meet military specifications. Therefore, at the request of the Air Force, a program was undertaken to improve the afterburner performance sufficiently to meet thrust specifications. Other phases of the XJ79 program are reported in references 1 and 2.

Some 13 afterburner configurations were investigated. Of these only nine were of major significance, and only the data for these nine are presented herein. The data presented illustrate the effects on performance of increased burner diameter and modifications to the flameholder, fuel

CONFIDENTIAL

injectors, and flow swirl into the afterburner. The data presented in references 3 to 6 and used as a guide to burner configurations shows the effects of similar afterburner alterations on performance and operational characteristics.

Data were obtained over a range of afterburner fuel-air ratios at a burner-inlet temperature of 1530° R, and a range of burner-inlet pressures from 860 to 3290 pounds per square foot absolute. These conditions correspond to flight Mach numbers from 1.16 to 2.0 at altitudes from 35,000 to 70,000 feet. Graphical comparisons of performance are presented in terms of combustion efficiency, burner-outlet gas temperature, and burner pressure loss. Tabulated performance data are presented in tables I and II.

APPARATUS

Installation

The XJ79 installation in the altitude test chamber is shown in figure 1. The forward bulkhead, which incorporates a labyrinth seal around the engine-inlet air duct, was used to separate the engine-inlet air from the exhaust and to provide a means of maintaining a pressure difference across the engine. A bulkhead butterfly valve was used to control the amount of air used to ventilate the test chamber.

Engine

The XJ79 engine, used in this investigation, has a sea-level static thrust rating without afterburning of approximately 10,000 pounds at an engine speed of 7460 rpm. At this rating, the turbine-outlet gas temperature is 1070° F, and engine airflow is approximately 164 pounds per second.

Main components of the engine include a 17-stage axial-flow compressor which incorporates variable inlet guide vanes and first six stages of stator blades, a cannular-type combustor with ten cans, a three-stage turbine, a diffuser assembly, an afterburner with louvered cooling liner, iris-type variable primary and secondary nozzles, and a combination electronic and hydraulic control. For the purposes of this investigation, the secondary-nozzle segments were removed. During the investigation, the third-stage turbine-rotor design was changed slightly.

The control systems on the XJ79 engine comprise the main fuel system which incorporates the variable-stator control, an afterburner fuel system, and an exhaust-nozzle area control. The inputs to the main fuel control are manually selected throttle position, engine speed, compressor-inlet temperature, compressor-discharge pressure, and teleflex feedback

signal from the variable stators. To provide surge margin during acceleration and low corrected-speed operation, the inlet guide vanes and the first six stator stages are varied approximately 35° according to a corrected-engine-speed schedule. During the course of the investigation the schedule was altered and the maximum mechanical engine speed was raised 3 percent to 7700 rpm to achieve a higher thrust during operation at a high engine-inlet temperature corresponding to the Mach 2.0 flight condition. The original and altered variable-stator schedule is shown in figure 2.

The XJ79 afterburner fuel control system is a flow-scheduling type which schedules the required flow as determined by compressor-discharge pressure and throttle position. This fuel control system was not used during this investigation. The afterburner-fuel-flow schedule is presented in figure 3, and a schematic drawing of the afterburner fuel system used in the investigation is shown in figure 4. A flow divider and selector valve were provided to distribute the fuel for the required primary- and secondary-uniform patterns, and sector patterns. For this investigation the selector valve was actuated manually. Normally, fuel always flows through the primary sector set of fuel bars when the throttle is advanced to the afterburning position. Then, if the total flow required is greater than approximately 3300 pounds per hour, the secondary sector set of fuel bars becomes operative. When the throttle is further advanced, the primary-uniform and (depending on the total flow required) the secondary-uniform manifolds are supplied.

The exhaust-nozzle-area control mechanically schedules the exhaust-nozzle area as a function of throttle travel. The electronic temperature control, which receives the signal from twelve paralleled thermocouples at the turbine outlet, can override the mechanical schedule to open the nozzle area whenever necessary. This feature was used during part of the investigation. For the remainder of the program, the nozzle was manually controlled.

Afterburner Components

Afterburners of two different diameters were used during the investigation, one with a 33.7-inch outside diameter and the other with a 35.7-inch outside diameter. Details of the burners are shown in figure 5. Both burners were about the same length, approximately 83 inches. The inner body of the diffuser and the first 10-inch section of the outer wall were the same. The open and closed limits of the nozzle area were about 4.83 and 2.30 square feet, respectively.

In order to reduce the whirl of the gases leaving the turbine, 36 equally spaced antiwhirl vanes were installed at the inlet to the diffuser for two configurations. Details of the vanes are given in figure 6(a), and a photograph of the vanes and also the vortex generators is shown in figure 6(b). The 28 vortex generators were supplied as part of the engine

4644

CI-1 back

and are shown in figure 5. Only one of the five engines used in the investigation did not have any vortex generators installed.

Six flameholders were used during the investigation. They differed in blockage, axial location in the burner, and number of V-gutters. Details of the flameholders are shown in figure 7, and the axial location and percent blockage are given in table III along with other configuration details.

The details of the 4 spray bar configurations are given in figure 8. The differences were in radial fuel distribution and number of spray bars.

Instrumentation

A cross section of the engine and the afterburner showing station locations and a tabulation of instrumentation at each station are given in figure 9. Pressure and temperature measurements at a 24.5-inch-diameter venturi in the inlet duct (station 1) were used to determine engine airflow.

The simulated flight condition was determined by the engine-inlet instrumentation at station 2. Diffuser-inlet conditions were obtained from six rakes located 4.25 inches downstream of the turbine (station 5). The angle of gas whirl across the passage was measured at the fuel bar location (station 5a) and also at a station 1.8 inches downstream of the turbine outlet with a specially designed whirl probe having two static orifices.

Diffuser-outlet or flameholder-inlet conditions were determined at station 6 approximately 11 inches downstream of the diffuser-inlet station for the first four configurations with the 33.7-inch-diameter pipe. However, for the four configurations with the 35.7-inch-diameter pipe and configuration 9, station 6 was moved to a plane 16 inches downstream of the diffuser-inlet station. It is designated as station 6a for these configurations.

The same instrument that enabled the computation of whirl angle at the fuel bar station (5a) also permitted the establishment of a velocity profile inasmuch as total pressure, static pressure, and temperature were also measured. When the actuators for this device failed, it was necessary to install a fixed total-pressure and thermocouple rake at station 5a along with two static wall taps for some configurations.

The exhaust-nozzle-inlet conditions (station 9) were surveyed about 12 inches upstream of the exit with a water-cooled total-pressure rake and a wall static pressure. The facility balance system was used to measure the thrust of the engine and afterburner combination. The symbols

and methods of calculation used in this report are presented in appendixes A and B, respectively.

PROCEDURE

The performance characteristics of most of the afterburner configurations were obtained over a range of afterburner fuel-air ratios at the following simulated flight conditions and diffuser-inlet total pressures:

Altitude, ft	Flight Mach number	Engine- inlet ram recovery	Engine- inlet temper- ature, °R	Average diffuser- inlet total pressure, lb/sq ft abs
35,000	1.16	100	500	2800
45,000	1.16	100	500	1665
55,000	1.16	100	500	990
45,000	2.0	85	705	3250
58,000	2.0	85	705	1660
70,000	2.0	85	705	932

The procedure for obtaining steady-state-performance data was as follows:

After starting the engine and accelerating to rated speed (7460 rpm at all flight conditions for the first four configurations; for the remainder of the investigation, however, the engine speed was increased to 7700 rpm at the high Mach-number condition), the engine-inlet pressure and temperature and the rated turbine-outlet temperature were set at the proper conditions. The afterburner was then ignited by the "pilot" burner which contained its own fuel and sparkplug. The exhaust nozzle was opened manually and the afterburner fuel flow was regulated so that turbine-outlet temperature was maintained at the rated value of 1070° F. After burning was stable, the pilot burner was turned off, and steady-state data points were taken over the operable range of afterburner fuel-air ratios from lean blowout to open exhaust nozzle or rich blowout. Most of the data were obtained with uniform distribution of fuel flow. Some of the data, however, were taken with sector distribution.

RESULTS AND DISCUSSION

33.7-Inch-Diameter Burner

Diffuser performance. - The 33.7-inch-diameter burner will hereafter be referred to as the "small" burner. The diffuser performance of the prototype small burner of the manufacturer was evaluated, and the results are presented in figure 10 in the form of velocity profiles at various stations in the diffuser. The stations are 4.25, 9.5, and 15.0 inches downstream of the diffuser-inlet flange. The two downstream stations correspond to diffuser area ratios of 1.26 and 1.54, respectively. The data presented were obtained at a simulated flight condition of 35,000 feet and a flight Mach number of 1.16. The average diffuser-inlet (station 5) velocity was over 900 feet per second. At the flameholder inlet (15-inch, station 6), which was about 6 inches upstream of the flameholder in configuration 1, the velocity varied from 300 to a maximum of over 800 feet per second. Consideration of further diffusion shows that a peak velocity of approximately 675 feet per second would be reached near the flameholder. Previous experience (refs. 3, 5, and 6) indicates that peak velocities of this magnitude would contribute to high-pressure losses and reduced combustion efficiencies. The installation of the vortex generators did not significantly affect the velocity profile.

Over-all burner performance. - The prototype small-afterburner (configuration 1) performance is presented in figure 11. Afterburner total temperature and combustion efficiency are presented as functions of unburned-air fuel-air ratio, and the burner total-pressure drop as a function of burner temperature ratio. Although the exhaust-nozzle diameter was opened to 29 inches, the final burning temperature was only 3150° R; the combustion efficiency was 73 percent and the pressure loss was about 15 percent.

This performance was poor compared with previous afterburner experience (refs. 3 to 6). Two areas of improvement were obvious: (1) reduce flameholder and spray bar blockage to lower pressure loss and thus permit higher gas temperatures, and (2) improve fuel distribution to raise combustion efficiency. Configuration 2 incorporated these improvements and the performance was raised as expected.

A 30-percent blockage two-V-gutter flameholder was installed, and the 40 individual fuel spray bars were combined into 20 tandem bars of the same frontal area with new orifice spacing to more nearly match the air distribution.

The performance comparison of configurations 1 and 2 are presented in figure 12 for a flight condition of 35,000 feet, and a Mach number of 1.16. The peak temperature was raised to 3600° R for configuration 2. Peak combustion efficiency was raised to 92 percent. The total-pressure

drop across the burner decreased 0.035 points. The decreased spray bar blockage accounted for only about 10 percent of the difference in pressure drop.

Configuration 2 represented the most significant performance change of the small and large burner configurations, and the other configurations were run to develop additional minor improvements and to check out possible prototype alternates.

Configurations 3 and 4 were run to evaluate the effects of two variables for an impending Mach 2.0 flight of a prototype airplane which had a 30-percent blockage three-V-flameholder. The first variable evaluated was the flameholder position. Configuration 3 had the flameholder mounted 11.4 inches downstream of the fuel spray bars, and configuration 4 had the flameholder mounted 5 inches further downstream. The other variable evaluated was a change in the variable stator schedule. For an engine-inlet temperature of 705° R at an engine speed of 7460 rpm, the corrected engine speed is approximately 6400 rpm. The variable stator schedule (fig. 2) calls for an angle of about 9°. In order to increase mass flow at this condition, the manufacturer requested that angles of 0° and 5° be run for both configurations.

The performance of configurations 3 and 4 is presented in figure 13 for an altitude of 58,000 feet. The downstream location of the flameholder gives a higher final temperature and combustion efficiency, and a lower pressure drop. The 5° variable stator position provides about 3.5 percent less mass flow and also shows an advantage in higher combustion efficiency and lower pressure drop. However, since the lower flow will penalize thrust, it becomes necessary to compare the configurations on a specific fuel consumption against net thrust basis. In order to provide a comparison with the specification of the manufacturer (ref. 7), it is necessary to adjust the data for the performance of an ejector nozzle with 7-percent secondary air and 100-percent ram recovery engine-inlet conditions. (The experimental ejector-nozzle performance taken from refs. 1 and 2 is shown in fig. 25.)

This comparison between configurations 3 and 4 is presented in figure 14 for a flight condition of 61,400 feet, and a Mach number of 2.0. The 3.5 percent lower airflow for the 5° variable stator position more than offsets the effect of higher combustion efficiency and lower pressure drop for both configurations. Thus the 0° variable stator position shows up with the highest maximum net thrust and the lowest specific fuel consumption.

35.7-Inch-Diameter Burner

The engine had not reached the specification level at the Mach 2.0 condition. One of the most direct ways to improve the afterburner

performance in order to achieve the specification thrust was to increase the burner diameter, and, therefore, lower the burner velocity. The lower velocity would reduce pressure losses and permit higher gas temperatures and, consequently, higher thrust for the same exhaust nozzle. The manufacturer provided a burner with a 2-inch larger diameter which gave a 12-percent increase in cross-sectional area. In addition, a "reset" feature was incorporated in the engine fuel control to allow the engine speed to increase to 7700 rpm, to increase mass flow (and thrust) and the variable stators, and to assume a 2° position when the inlet temperature approached 705°R (corrected engine speed equals 6600 rpm). Also, a slightly modified third-stage turbine-rotor design was incorporated at this time.

Diffuser Performance

The 35.7-inch-diameter burner will hereafter be referred to as the "large" burner. The diffuser performance of the large burner was evaluated, and the results are presented in figure 15. The stations are 4.25 and 20 inches downstream of the diffuser-inlet flange. The downstream station 6 had a diffuser area ratio of 1.7. As shown in figure 15(a) for a flight condition of 35,000 feet and a Mach number of 1.16, the average diffuser-inlet velocity (station 5) was about 900 feet per second, but the profile is somewhat flatter than the one for the original engine (fig. 10). This flatness is probably due to the slight change in the third-stage turbine-rotor design. At the downstream station 6, which was about 3 inches upstream of the flameholder for configurations 5 to 8, the velocity peak was still about 640 feet per second. At a flight condition of 70,000 feet and a Mach number of 2.0, the corrected engine speed drops to 6600 as explained previously. The velocity profiles through the diffuser at this condition are presented in figure 15(b). The peak diffuser-inlet (station 5) velocity is much higher at Mach 2.0 than that for the 1.16-Mach-number case. The peak flameholder-inlet station 6a velocity has also risen to almost 700 feet per second.

The whirl patterns existing at the turbine outlet for the earlier engines had exhibited some maximum angles of 15° . However, as shown in figure 16 for a station 1.8 inches downstream of the turbine, the maximum whirl angle increased to over 20° . Therefore, in an effort to improve combustion efficiency and reduce over-all pressure losses, a set of anti-whirl vanes were installed for configurations 6 and 7. The maximum whirl angle was reduced to less than 10° . The velocity profile behind the vanes did not change markedly except for a lower velocity behind the inner support ring (see fig. 7(a)). For a production design, the vane assembly could undoubtedly be improved, that is, streamlining of the vanes and supports and elimination of the bolts and nuts protruding into the airstream. The total-pressure loss across the vanes amounted to 2 percent at a Mach number of 1.16 and 3 percent at a Mach number of 2.0.

Over-All Burner Performance

Configuration 5 consisted of configuration 2 geometry adapted to the large burner which represented the best design practice on the basis of reference 5. The performance of configurations 2 and 5 is compared in figure 17 at the reference flight condition of 35,000 feet and Mach number of 1.16. As shown in figure 17, the main objectives of the larger burner diameter were attained, that is, lower pressure drop and, therefore, higher temperature for the same exhaust-nozzle area. The lower combustion efficiency at low fuel-air ratio is not a basic fault of the large burner, but is due to the fact (1) that detailed tailoring of the fuel distribution to optimize combustion efficiency was prevented by lack of time, and (2) that more turbine-outlet swirl was present for the large burner. (This swirl probably was due to the slight design change in the third-stage turbine rotor.)

The antiwhirl vanes were installed at this time to find a possible improvement. The performance comparison of configurations 5 and 6 is presented in figure 18. Both temperature and combustion efficiency are higher for configuration 6. The burning pressure drop is identical. However, an additional 2 percent must be added to the pressure-drop values plotted for configuration 6 to account for the loss across the vanes since they are ahead of the diffuser-inlet station.

An aerodynamically clean design of the vanes would cut the pressure drop and improve the thrust and specific fuel consumption. The complication and weight would have to be considered to determine their net worth.

Since the velocity profile was changed slightly with the wake behind the vane support rings, some damage occurred to the burner skin. The fuel distribution was therefore altered to keep the fuel away from the skin. This was accomplished by replacing spray bars C with D. A performance comparison of configurations 6 and 7 is presented in figure 19 to show the effect of fuel distribution.

The final burning temperature for configuration 7 dropped 100° to 200° R, and the combustion efficiency also fell lower by 3 to 7 percent. The pressure drop remained the same. The results indicate that the fuel distribution was changed more radically than it should have been just to help the cooling problem.

Again, because the manufacturer was more interested in a three-V-gutter flameholder for prototype purposes, a flameholder of this type with V-gutters connecting the rings was installed, and the antiwhirl vanes were removed. The results of this evaluation are compared with those of the two-V-gutter flameholder (configuration 5) in figure 20(a) for the 1.16 flight Mach number and in figure 20(b) for the 2.0 flight Mach number. The combustion efficiency and temperature are higher for configuration 8

(three-V-gutter flameholder) for a flight condition of 35,000 feet and a Mach number of 1.16, while the pressure drop is slightly lower. The comparison at a flight Mach number of 2.0, however, is not so clear cut. The pressure drop is essentially the same at all three altitudes of 45,000, 58,000, and 70,000 feet. The combustion efficiency for configuration 5, the two-V-gutter flameholder, is higher at 58,000 and 70,000 feet and (for the one data point available) lower at 45,000 feet. On the basis of the available data, configuration 8 (three-V-gutter flameholder) was picked by the manufacturer for the final configuration.

The manufacturer had developed the sector-burning principle (where fuel is injected into only two opposite 90° quadrants) with the philosophy that locally fuel-rich regions would allow the burner to operate at a lower total fuel-air ratio than uniform fuel injection. Light-offs (afterburner starts) would be smoother and lean blowouts would be less violent for the control system. Therefore, for the final large burner configuration, this variable was investigated only at the 1.16 flight Mach-number condition. The results are presented in figure 21. The combustion efficiency and temperature are higher for the sector burning at the low fuel-air-ratio range. Then, as the local sector fuel-air ratio goes above stoichiometric, the efficiency drops off as expected.

As shown in figure 22, the operational limits do show some advantage for the sector system in lowering the lean blowout limits.

For some airframe applications, the large-diameter burner could not be tolerated for space requirement reasons. Therefore, the manufacturer planned to put one version of each burner into production. A direct comparison of the performance level of the two production versions was obtained. The final small-burner configuration consisted of the same design fuel spray bars and a scaled-down version of the configuration 8, three-V-gutter flameholder. The performance comparison is presented in figure 23(a) for the 1.16 flight Mach number and in figure 23(b) for the 2.0 flight Mach number.

At all flight conditions, the combustion efficiency and temperature are higher, and the pressure drop is lower for the large burner. In fact, the small-burner production configuration had 10 percent lower combustion efficiency and about 1 percent higher pressure loss than configuration 2. The exhaust-nozzle diameters noted on figure 23(b) indicate that the nozzle was opened at a lower fuel-air ratio for the small burner. This fact, plus the large pressure-loss difference make it mandatory that the final comparison should be on a thrust and specific-fuel-consumption basis.

When the program was nearing completion, the engine capabilities had been reevaluated by the manufacturer, and a new thrust and specific-fuel-consumption specification established. Reference 8 was therefore used as a basis for final comparison of the small- and large-burner configurations.

This new specification requires an ejector using 8-percent secondary air and assumes an inlet recovery specified by A.I.A. (This curve is shown in fig. 5.) The experimental data have been adjusted for the 8-percent secondary airflow by the thrust coefficient (shown in fig. 26).

The variation of specific fuel consumption with net thrust is presented in figure 24 for the large- and small-burner adjusted data and cross-plotted specification data at a flight condition of 59,400 feet and a Mach number of 2.0. Both burners exceeded the revised specification for the specific fuel consumption. However, the small burner failed to meet the revised thrust specification by 100 pounds. The reevaluation of the engine was significant in that neither configuration met the original specification. At a net thrust of 4000 pounds, the specific fuel consumption for the large burner is 10 percent lower than the small burner. The maximum thrust of the large burner is 19 percent greater than the small burner.

SUMMARY OF RESULTS

The results of evaluating several afterburner configurations on an XJ79 engine are as follows:

1. Simple fuel system and flameholder modifications to the original configuration raised the combustion efficiency and lowered the pressure drop resulting in substantial thrust increases. Applying these modifications to a larger-diameter burner resulted in further performance gains at all flight conditions investigated. A performance comparison of the final large- and small-burner configurations show that at 59,400 feet and a Mach number of 2.0, the thrust advantage for the large burner amounted to 19 percent, and the specific fuel consumption was lower by approximately 10 percent.

2. Antiwhirl vanes reduced the whirl significantly and increased the combustion efficiency an average of 2.5 percent over the higher fuel-air-ratio range. This small increase probably would not merit the added complication and increased pressure drop. A comparison of two-V-gutter and three-V-gutter 30-percent blockage flameholders in a 35.7-inch-diameter burner revealed little variation in performance over a wide range of flight conditions. Enriching the center of the burner by moving the fuel-bar injection holes inward relative to the air distribution lowered the combustion efficiency by approximately 7 percent over the range of operable fuel-air ratios at 35,000 feet and a Mach number of 1.16.

Sector burning, investigated with prototype configuration in the large burner, provided leaner over-all fuel-air lean blowouts than uniform

4644

CI-2, back

burning, and also provided higher combustion efficiency at the lower fuel-air-ratio range. In the higher fuel-air-ratio range, sector burning provided no advantage.

Lewis Flight Propulsion Laboratory
National Advisory Committee for Aeronautics
Cleveland, Ohio, September 23, 1957

4644

APPENDIX A

SYMBOLS

A	cross-sectional area, sq ft
a	speed of sound
B	thrust-cell force, lb
C_D	flow coefficient, ratio of actual flow to flow calculated at nozzle throat
C_V	velocity coefficient, ratio of actual jet velocity to effective jet velocity
d	diameter, in.
F_j	jet thrust, lb
F_{ip}	ideal jet thrust obtained from complete expansion of primary nozzle total pressure to ambient pressure, lb
F_{ej}	ejector nozzle jet thrust, lb
F_n	net thrust, lb
f	fuel-air ratio
g	acceleration due to gravity, 32.2 ft/sec ²
M	Mach number
N	engine speed, rpm
P	total pressure, lb/sq ft abs
p	static pressure, lb/sq ft abs
R	gas constant, 53.4 (ft)(lb)/(lb) °R
T	total temperature
V	velocity, ft/sec
w_a	airflow, lb/sec

w_f fuel flow, lb/hr
 w_f/F_n specific fuel consumption based on total fuel flow and net thrust,
(lb)/(hr)(lb thrust)
 w_g gas flow, lb/sec
 γ ratio of specific heat for gases
 η efficiency
 τ afterburner total-temperature ratio

Subscripts:

a air
ab afterburner
ac actual
b bleed
d duct
e engine
eff effective
f fuel
g gas
id ideal
n exhaust nozzle
p primary system
R rake
sc scale
t total
ua unburned air
O free-stream conditions
1 engine airflow measuring station

- 2 engine-inlet station
- 5 diffuser-inlet station
- 6 flameholder-inlet station
- 9 tailrake station

APPENDIX B

METHODS OF CALCULATION

Airflow. - Airflow was determined from pressure and temperature measurements obtained in the engine-inlet duct. These measurements were used in the following equation:

$$\frac{PA}{w_a \sqrt{gRT}} = \frac{\left(\frac{P}{p}\right)^{1/\gamma}}{\sqrt{\frac{2\gamma}{\gamma-1} \left[1 - \left(\frac{p}{P}\right)^{\frac{\gamma-1}{\gamma}}\right]}}$$

The right hand side of the previous equation is listed as a function of p/P in reference 9. Simple rearrangement of the equation then yields airflow.

Airflow at station 5 (diffuser inlet) was determined from

$$w_{a,5} = 0.997 w_{a,1} - w_{a,b}$$

The 0.997 factor was determined from the estimated leakage obtained from the manufacturer. Instrumentation in bleed stacks that vented compressor leakage air measured $w_{a,b}$.

Gas flow. - Gas flow was obtained by adding the total fuel flow to the airflow at station 5

$$w_{g,9} = w_{a,5} + \frac{w_{f,t}}{3600}$$

Equivalence ratio. - Equivalence ratios were determined as follows:

$$S = \frac{f}{f_{st}}$$

where S is the equivalence ratio and the subscript st , stoichiometric.

For the fuel investigated herein,

$$f_{st} = 0.06745$$

Therefore,

$$S_{t,ac} = \frac{W_{f,e} + W_{f,ab}}{W_{a,5} (0.06745)}$$

where $S_{t,ac}$ is the actual equivalence ratio based on total fuel flow.

Fuel-air ratio. - Fuel-air ratio based on unburned air was found by

$$f_{ua} = 0.06745 \left(\frac{S_{t,ac} - S_{e,id}}{1 - S_{e,id}} \right)$$

where $S_{e,id}$ is the ideal equivalence ratio for the temperature rise from engine-inlet to diffuser-inlet stations (shown in a table in ref. 10).

Combustion efficiency. - Combustion efficiency was then determined by

$$\eta_{ab} = \frac{f_{id}}{f_{t,ac}} = \frac{S_{id}}{S_{t,ac}} = \frac{S_{t1} - S_{e,id}}{S_{t,ac} - S_{e,id}}$$

where S_{t1} is the ideal equivalence ratio for the temperature rise from engine inlet to tailpipe exit (shown in a table in ref. 10).

Jet thrust. - Scale jet thrust was determined from the facility thrust cell and the pressure force across the seal area A_s .

$$F_j = B + A_s(P_1 - P_0)$$

Velocity coefficient. - Velocity coefficient was determined from nonburning data as follows:

$$C_V = \frac{F_{j,sc}}{F_{j,R}} = \frac{B + A_s(P_1 - P_0)}{\sqrt{\frac{R}{g}} w_{g,9} \frac{V_{eff}}{\sqrt{gRT_9}} \sqrt{T_9}}$$

$$(C_V = 0.99 \text{ for the range of data obtained})$$

where V_{eff}/\sqrt{gRT} is an effective velocity parameter which is a function of P_0/P_9 and γ (ref. 9).

Gas temperature. - Afterburner total temperature was calculated as follows:

$$T_{ab} = \left[\frac{F_j / C_v}{\sqrt{\frac{R}{g}} w_{g,9} \frac{V_{eff}}{\sqrt{gRT}}} \right]$$

Flight Mach number. - Mach number was calculated from engine-inlet conditions and an assumed total-pressure loss.

$$M_0 = \sqrt{\frac{2}{\gamma - 1} \left[\left(\frac{P_0}{P_0} \right)^{\frac{\gamma-1}{\gamma}} - 1 \right]}$$

where $P_0 = P_2 / \eta_d$.

Diffuser-inlet Mach number. - Mach number was determined from the measured quantities $w_{g,5}$, T_5 , P_5 , and A_5 and the following equation, assuming a 0.9 area coefficient for the flow passage:

$$\frac{w_{g,5} T_5}{A_5 P_5} \frac{R}{rg} = \frac{M}{\left(1 + \frac{\gamma - 1}{2} M^2 \right)^{\frac{\gamma+1}{2(\gamma-1)}}}$$

The right side of this equation is listed as a function of M and γ in reference 11 where $\gamma = 1.34$ should be used for diffuser-inlet conditions. The measured static pressure at station 5 checked very closely with a calculated static pressure which was obtained from the pressure ratio p/P listing in reference 11.

Diffuser velocity profiles. - With the use of an actuated probe that measured total pressure, static pressure, and temperature across the passage at a given station, velocity could be calculated using the same reference 11 and the following equations:

$$\frac{p}{P} = \left(1 + \frac{\gamma - 1}{2} M^2 \right)^{-\frac{\gamma}{\gamma-1}}$$

and

$$M = \frac{V}{a_t}$$

$$a_t = \sqrt{\gamma g R T}$$

When static pressure was not measured, it was calculated as explained in the diffuser-inlet Mach-number calculation, and a flat profile was assumed.

Net thrust. - Net thrust for comparison with the engine specification of the manufacturer was calculated in the following manner:

1. A flight condition was picked from the engine-inlet total pressure of the experimental data and the ram recovery for the particular specification.

For example, at a Mach number of 2.0, η_d is 0.90 as shown in figure 25 (ref. 8). (In ref. 7, $\eta_d = 1.00$.) So that,

$$P_0 = \frac{P_2}{\eta_d} = \frac{1080}{0.90} = 1211$$

At a Mach number of 2.0, $p_0/P_0 = 0.12780$ and, therefore,

$$p_0 = (0.1278)(1211) = 154.6$$

which corresponds to an altitude of 59,400 feet.

2. Then, an ideal jet thrust was calculated from

$$F_{ip} = \sqrt{\frac{R}{g}} w_{g,9} \sqrt{T_{ab}} \frac{V_{id}}{\sqrt{gRT}}$$

where V_{id}/\sqrt{gRT} is an ideal velocity parameter which is a function of p_0/P_9 (ref. 9).

3. By using the ejector performance curve, F_{ej}/F_{ip} was obtained for the proper secondary airflow and primary diameter. From reference 8, $w_s/w_p = 0.08$ (ref. 7, $w_s/w_p = 0.07$) as shown in figure 26.

$$F_{ej} = \frac{F_{ej}}{F_{ip}} (F_{ip})$$

4. Finally net thrust was obtained

$$F_n = F_{ej} - 1.08 M_a V_0$$

4644

CI-3 back

where $1.08 = 1 + \text{secondary-flow percentage}$, and $V_0 = 1942$ feet per second for $M_0 = 2.0$. An alternate method for calculating net thrust may be employed if the tank ambient pressure p_{tank} equals the ambient pressure p_0 calculated. The scale jet thrust must be adjusted to ideal jet thrust by the following:

$$F_{ip} = \frac{F_{j,sc}}{C_v C_D} \frac{V_{id}}{V_{eff}}$$

The ratio V_{id}/V_{eff} may be obtained from reference 9, and C_D was obtained from nonburning data (choked flow)

$$C_D = \frac{w_{g,9}}{\frac{P_9 A_n}{\sqrt{T_9}} \sqrt{\frac{\gamma}{R}} \left(\frac{2}{\gamma + 1} \right)^{\frac{\gamma+1}{2(\gamma-1)}}$$

($C_D = 0.99$ for the range of data obtained.) Then the steps 3 and 4 may be calculated to obtain net thrust.

REFERENCES

1. Greathouse, William K., and Bloomer, Harry E.: Preliminary Internal Performance Data for a Variable-Ejector Assembly on the XJ79-GE-1 Turbojet Engine. I - Nonafterburning Configurations. NACA RM E56E23, 1956.
2. Bloomer, Harry E., and Groesbeck, Donald E.: Preliminary Internal Performance Data for a Variable-Ejector Assembly on the XJ79-GE-1 Turbojet Engine. II - Afterburning Configurations. NACA RM E57F25, 1957.
3. King, Charles R.: Experimental Investigation of Effects of Combustion-Chamber Length and Inlet Total Temperature, Total Pressure, and Velocity on Afterburner Performance. NACA RM E57C07, 1957.
4. Nakanishi, Shigeo, and King, Charles R.: Effect of Some Configuration Changes on Afterburner Combustion Performance. NACA RM E57C01, 1957.
5. Lundin, Bruce T., Gabriel, David S., and Fleming, William A.: Summary of NACA Research on Afterburners for Turbojet Engines. NACA RM E55L12, 1956.

6. Prince, William R., Velie, Wallace W., and Braithwaite, Willis M.: Full-Scale Evaluation of Some Flameholder Design Concepts for High-Inlet-Velocity Afterburners. NACA RM E56D10, 1956.
7. Parker, D. E., and Jacobs, E. S.: Estimated Minimum Performance of the General Electric J79 Turbojet Engine. Bull. No. R55AGT400, Aircraft Turbine Div., General Electric Co., Oct. 2, 1955.
8. Buck, T. F., and Bailey, E. E.: Estimated Minimum Performance of the General Electric J79 Phase I Turbojet Engine. Bull. R56AGT129, Aircraft Turbine Div., General Electric Co., Sept. 15, 1956.
9. Turner, L. Richard, Addie, Albert N., and Zimmerman, Richard H.: Charts for the Analysis of One-Dimensional Steady Compressible Flow. NACA TN 1419, 1948.
10. Huntley, S. C.: Ideal Temperature Rise Due to a Constant-Pressure Combustion of a JP-4 Fuel. NACA RM E55G27a, 1955.
11. Lewis Laboratory Computing Staff: Tables of Various Mach Number Functions for Specific-Heat Ratios from 1.28 to 1.38. NACA TN 3981, 1957.

TABLE I. -

Run	Altitude, ft	Flight Mach number, M ₀ , nominal	Variable stator position, deg from open position	Engine speed, N, rpm	Compressor- inlet total temperature, T ₂ , °R	Compressor- inlet total pressure, P ₂ , lb sq ft abs	Tank ambient pressure, P _{tank} , lb sq ft abs	Diffuser- inlet total temperature, T ₅ , °R	Diffuser- inlet total pressure, P ₅ , lb sq ft abs	Tailrake total pressure, P _g , lb sq ft abs	Compressor- inlet airflow, lb/sec
(a) Configuration 3;											
18	58,000	2.0	0	7460	696	1092	199	1538	1595	1385	54.06
22	↓	↓	↓	7457	699	1086	194	1535	1584	1386	53.44
19	↓	↓	↓	7453	696	1094	187	1532	1585	1385	53.85
20	↓	↓	↓	7454	698	1094	192	1531	1590	1407	53.70
21	↓	↓	↓	7457	698	1095	190	1532	1582	1425	53.60
13	↓	↓	5	7465	701	1093	191	1522	1613	1409	51.76
14	↓	↓	↓	7475	699	1094	201	1516	1611	1414	52.06
15	↓	↓	↓	7459	700	1089	200	1522	1606	1421	51.80
16	↓	↓	↓	7460	702	1094	196	1517	1605	1436	51.50
17	↓	↓	↓	7458	698	1090	190	1521	1629	1481	51.82
(b) Configuration 4;											
11	58,000	2.0	0	7461	697	1093	172	1542	1599	1390	54.07
13	↓	↓	↓	7462	697	1085	177	1541	1599	1395	53.66
12	↓	↓	↓	7463	697	1087	173	1535	1597	1380	53.47
9	↓	↓	↓	7461	697	1087	186	1536	1577	1381	53.40
10	↓	↓	↓	7464	697	1093	184	1545	1594	1408	54.07
14	↓	↓	↓	7452	697	1090	159	1538	1594	1450	53.67
8	↓	↓	5	7458	697	1102	176	1538	1662	1467	52.64
3	↓	↓	↓	7459	698	1094	175	1529	1635	1445	51.80
7	↓	↓	↓	7455	697	1087	176	1532	1664	1481	52.65
4	↓	↓	↓	7484	696	1094	167	1537	1642	1470	52.15
5	↓	↓	↓	7452	697	1096	170	1533	1648	1495	52.41
(c) Configuration 2;											
3	35,000	1.16	0	7474	491	1146	504	1557	2953	2547	92.38
4	↓	↓	↓	7468	490	1143	503	1533	2947	2545	92.42
2	↓	↓	↓	7467	491	1140	499	1491	2808	2400	91.94
5	↓	↓	↓	7469	491	1146	505	1531	2944	2551	92.44
6	↓	↓	↓	7468	490	1144	500	1534	2956	2570	92.42
7	↓	↓	↓	7478	491	1145	498	1514	2911	2534	92.19
9	↓	↓	↓	7480	491	1148	504	1529	2953	2599	92.59
8	↓	↓	↓	7463	491	1146	503	1481	2854	2469	92.38
10	↓	↓	↓	7465	491	1144	503	1532	2956	2626	92.28
11	↓	↓	↓	7463	491	1146	508	1621	2933	2638	92.40
12	↓	↓	↓	7465	491	1149	504	1539	2964	2718	92.72
(d) Configuration 9; final;											
4	35,000	1.16	0	7466	500	1144	489	1524	2704	2317	89.58
3	↓	↓	↓	7470	500	1139	491	1523	2694	2305	89.15
6	↓	↓	↓	7464	503	1139	500	1499	2702	2322	89.07
9	↓	↓	↓	7460	498	1141	493	1504	2708	2346	89.21
5	↓	↓	↓	7463	499	1146	487	1505	2708	2351	89.75
7	↓	↓	↓	7463	503	1139	500	1509	2692	2365	89.70
6	↓	↓	↓	7480	499	1141	495	1507	2718	2417	89.37
10	↓	↓	↓	7469	497	1147	495	1512	2750	2464	90.60
38	45,000	2.00	2	7700	709	2063	305	1528	3006	2587	106.86
39	↓	↓	↓	7700	702	2057	299	1514	3018	2571	106.33
37	↓	↓	↓	7700	707	2052	312	1548	2997	2552	106.64
36	↓	↓	↓	7700	705	2052	311	1548	3014	2585	106.80
35	↓	↓	↓	7700	698	2047	305	1548	3075	2643	107.98
34	↓	↓	↓	7700	701	2037	311	1527	3025	2621	106.99
40	↓	↓	↓	7700	706	2044	283	1514	2966	2607	106.72
14	55,000	1.16	0	7446	508	440	186	1518	989	856	33.26
11	↓	↓	↓	7448	503	437	192	1522	993	861	33.74
13	↓	↓	↓	7445	508	437	193	1523	988	859	33.50
12	↓	↓	↓	7445	507	439	194	1523	995	868	33.50
18	↓	↓	↓	7444	503	438	191	1517	1000	875	33.58
17	↓	↓	↓	7444	504	438	190	1516	994	876	33.56
16	↓	↓	↓	7444	505	439	192	1514	991	875	33.65
15	↓	↓	↓	7444	507	439	187	1517	992	879	33.37
22	58,000	2.00	2	7704	704	1098	164	1536	1609	1361	57.18
25	↓	↓	↓	7700	708	1109	159	1548	1612	1370	56.98
23	↓	↓	↓	7701	705	1089	153	1536	1595	1351	56.15
21	↓	↓	↓	7703	700	1083	147	1531	1618	1369	57.61
24	↓	↓	↓	7702	709	1106	143	1537	1593	1372	56.46
26	70,000	↓	↓	7677	706	819	161	1550	873	736	30.74
27	↓	↓	↓	7679	708	822	155	1535	867	720	30.92
28	↓	↓	↓	7674	706	820	156	1548	862	731	30.74
29	↓	↓	↓	7675	707	821	155	1548	867	740	30.90
30	↓	↓	↓	7674	706	818	158	1545	861	739	30.87
31	↓	↓	↓	7670	707	823	158	1544	866	749	30.94
32	↓	↓	↓	7672	704	818	160	1540	862	750	30.73

4644

SMALL BURNER

Engine fuel flow, $W_{f,e}$, lb/hr	After- burner fuel flow, $W_{f,ab}$, lb/hr	Tail- pipe gas flow, $W_{g,p}$, lb/sec	Afterburner fuel-air ratio based on unburned air, f_{ua}	Jet thrust, F_j , lb	Calculated afterburner total temperature, $T_{n,OR}$	Exhaust- nozzle, diameter, D_n , in.	Afterburner combustion efficiency, η_{ab}	Burner total- pressure loss ratio, $\frac{P_5 - P_9}{P_5}$	Diffuser- inlet Mach number, M_5	Burner total- temperature ratio, T_D/T_5
three-V-flameholder (upstream)										
2235	11,345	56.08	0.0579	6,910	3472	29.63	0.733	0.132	0.54	2.257
2210	10,285	55.18	.0518	6,756	3404	29.20	.784	.125	.54	2.217
2220	10,345	55.69	.0516	6,742	3537	29.22	.755	.128	.54	2.177
2225	8,975	55.06	.0432	6,540	3165	28.40	.803	.115	.54	2.067
2220	7,670	54.59	.0349	6,040	2751	27.07	.714	.099	.54	1.795
2090	12,890	54.25	.0715	6,891	3633	29.20	.656	.127	.50	2.387
2095	11,520	54.16	.0618	6,730	3503	28.84	.703	.122	.50	2.311
2095	10,220	53.34	.0539	6,542	3407	28.33	.759	.115	.50	2.237
2080	8,850	52.86	.0441	6,346	3224	27.65	.821	.105	.50	2.125
2120	7,570	52.93	.0359	6,040	2854	26.39	.763	.091	.49	1.877
three-V-flameholder (downstream)										
2330	9,350	56.19	0.0599	7,074	3500	29.67	0.721	0.131	0.55	2.269
2340	9,040	55.70	.0585	6,992	3499	29.47	.736	.128	.55	2.271
2300	8,650	55.39	.0560	6,971	3500	29.44	.771	.130	.54	2.281
2315	7,875	55.10	.0513	6,838	3376	29.18	.779	.124	.55	2.197
2340	7,250	55.60	.0465	6,765	3216	28.65	.771	.117	.56	2.081
2315	5,840	54.82	.0379	6,506	3013	27.75	.618	.103	.55	1.959
2260	10,175	54.99	.0668	7,096	3636	28.79	.701	.117	.50	2.364
2235	9,200	53.88	.0616	6,940	3630	28.72	.759	.117	.50	2.373
2260	8,075	54.42	.0531	6,860	3452	28.11	.789	.110	.50	2.253
2245	7,220	53.68	.0480	6,708	3357	27.82	.820	.105	.50	2.183
2245	6,070	53.61	.0402	6,483	3132	27.05	.842	.093	.50	2.043
two-V-flameholder										
4670	16,700	96.38	0.0651	11,547	3614	28.81	0.752	0.138	0.60	2.321
4670	15,500	96.08	.0603	11,479	3593	28.81	.804	.136	.50	2.344
4400	15,370	95.50	.0593	11,310	3612	28.67	.832	.145	.52	2.423
4640	14,560	95.83	.0565	11,372	3543	28.65	.833	.134	.50	2.314
4640	13,750	95.59	.0534	11,326	3507	28.41	.863	.131	.49	2.286
4685	12,790	95.08	.0497	11,155	3450	28.42	.897	.130	.50	2.278
4640	11,550	95.15	.0447	11,006	3331	27.81	.923	.120	.49	2.178
4440	11,500	94.87	.0442	10,795	3291	28.42	.917	.129	.51	2.222
4660	10,250	94.48	.0399	10,697	3163	27.19	.921	.112	.49	2.064
4605	8,525	94.11	.0350	10,073	2822	26.27	.857	.101	.50	1.856
4725	6,980	94.02	.0270	9,511	2472	25.00	.736	.089	.49	1.808
three-V-flameholder										
4430	16,740	94.26	0.066	11,092	3546	29.87	0.708	0.143	0.54	2.33
4395	16,620	93.87	.066	11,033	3548	29.87	.712	.144	.54	2.33
4415	15,300	93.39	.061	10,981	3532	29.36	.765	.141	.53	2.36
4425	13,920	93.15	.055	10,911	3448	28.96	.799	.134	.53	2.29
4430	12,880	93.34	.050	10,764	3318	28.67	.816	.131	.54	2.20
4375	10,315	91.60	.041	10,116	3044	27.85	.818	.118	.54	2.02
4445	9,100	91.96	.036	9,946	2883	27.06	.822	.111	.53	1.91
4495	8,070	92.92	.032	9,710	2671	26.38	.782	.104	.53	1.77
4505	13,355	110.25	.043	13,445	3199	29.64	.824	.146	.60	2.09
4550	13,005	111.36	.041	13,594	3208	29.95	.865	.148	.60	2.12
4495	12,765	109.90	.041	13,266	3142	29.36	.827	.149	.60	2.03
4530	12,220	109.90	.039	13,249	3100	29.02	.838	.142	.60	2.00
4680	11,980	110.73	.039	13,388	3081	28.73	.844	.141	.59	1.99
4580	10,845	109.53	.035	12,873	2918	28.43	.819	.134	.60	1.91
4430	8,690	108.42	.028	11,996	2530	27.39	.716	.121	.61	1.67
1685	6,525	35.09	.070	3,947	3237	28.08	.549	.134	.55	2.13
1695	5,790	35.56	.061	3,922	3165	28.80	.598	.133	.56	2.08
1675	5,185	34.78	.056	3,805	3082	28.50	.624	.131	.55	2.03
1675	4,990	34.89	.053	3,806	3056	28.31	.658	.128	.55	2.01
1695	4,535	34.85	.048	3,750	2950	27.86	.638	.125	.55	1.93
1685	3,935	34.67	.042	3,596	2714	27.34	.612	.119	.55	1.79
1675	3,625	34.67	.038	3,513	2604	26.98	.603	.117	.56	1.72
1685	3,325	34.31	.036	3,485	2584	26.54	.634	.114	.55	1.70
2470	7,300	58.96	.044	7,147	3160	29.46	.780	.134	.60	2.06
2440	6,980	58.60	.042	7,092	3107	29.10	.778	.130	.60	2.01
2450	6,440	57.71	.040	6,908	3016	28.90	.774	.148	.60	1.98
2430	5,755	58.85	.035	6,857	2805	28.42	.747	.142	.60	1.83
2430	5,505	57.63	.034	6,679	2757	28.09	.733	.139	.60	1.79
1355	4,685	32.09	.053	3,489	3072	29.88	.610	.157	.60	1.98
1320	4,300	32.15	.048	3,418	2914	29.89	.596	.160	.62	1.90
1320	4,285	31.96	.048	3,459	2989	29.51	.630	.162	.62	1.93
1330	3,975	32.04	.044	3,425	2877	29.08	.624	.147	.61	1.86
1330	3,675	31.62	.042	3,346	2830	28.71	.638	.142	.61	1.83
1325	3,475	31.92	.039	3,295	2666	28.37	.569	.135	.62	1.73
1330	3,290	31.66	.037	3,229	2611	27.95	.583	.130	.61	1.70

TABLE II. -

Run	Altitude, ft	Flight Mach number, M ₀ , nominal	Variable stator position, deg from open position	Engine speed, N, rpm	Compressor- inlet total temperature, T ₂ , °R	Compressor- inlet total pressure, P ₂ , lb sq ft abs	Tank ambient pressure, P _{tank} , lb sq ft abs	Diffuser- inlet total temperature, T ₅ , °R	Diffuser- inlet total pressure, P ₅ , lb sq ft abs	Tailrake total pressure, P ₉ , lb sq ft abs	Compressor- inlet airflow, lb/sec
(a) Configuration 5;											
4-2	35,000	1.16	1	7470	512	1152	510	1487	2773	2468	89.78
4-4			1	7474	503	1148	508	1486	2799	2502	90.81
7			0	7477	496	1154	500	1503	2869	2567	92.45
6			0	7478	496	1154	495	1503	2869	2578	92.58
5			0	7475	496	1154	489	1513	2876	2599	92.82
4			0	7468	497	1152	490	1514	2877	2613	92.28
3			0	7478	498	1152	494	1512	2868	2615	91.97
2			0	7474	498	1156	493	1503	2861	2623	92.30
8			0	7467	494	1151	488	1509	2864	2638	92.10
4,5			1	7488	503	1145	507	1486	2802	2588	90.70
4,5			1	7472	507	1152	492	1490	2804	2592	90.53
9			0	7487	493	1161	497	1506	2855	2645	92.90
4-8	45,000	2.00	2	7740	703	2065	294	1536	3330	2924	114.44
4-6	58,000	1.16	1	7466	503	371	179	1513	894	809	29.72
4-7		1.16	1	7463	503	359	181	1524	961	773	28.44
12		2.00	2 $\frac{1}{2}$	7681	703	1101	206	1555	1777	1557	60.17
11			2 $\frac{1}{2}$	7688	699	1095	204	1551	1788	1557	60.07
10			2	7688	702	1091	204	1549	1757	1573	60.92
14	70,000		2	7685	704	619	190	1558	947	822	32.87
15			2	7688	701	617	183	1555	948	831	33.15
(b) Configuration 6; two-V-flameholder;											
2	35,000	1.16	0	7457	507	----	500	1582	2860	2577	89.27
3			0	7460	507	----	481	1571	2850	2564	89.57
4			0	7460	507	----	478	1571	2850	2564	89.87
5			0	7460	508	----	464	1568	2825	2563	89.80
6			0	7455	508	----	407	1565	2825	2580	89.72
7			0	7483	509	----	488	1566	2818	2589	89.60
8			0	7456	507	----	494	1570	2824	2618	89.74
10	45,000	2.00	2.0	7731	704	----	329	1566	3266	2657	113.10
11			2.0	7735	709	----	322	1551	3235	2624	112.30
(c) Configuration 7; two-V-flameholder; antiswirl											
9	35,000	1.16	0	7453	516	1140	510	1522	2664	2380	88.06
8			0	7452	517	1143	502	1519	2661	2375	88.13
7			0	7459	517	1137	503	1513	2656	2376	87.86
6			0	7463	517	1135	504	1514	2657	2392	87.68
5			0	7451	517	1138	488	1508	2660	2411	87.77
4			0	7449	518	1137	492	1509	2642	2415	87.81
10			0	7451	516	1139	517	1524	2697	2508	88.06
15	45,000	2.00	2.0	7705	710	2031	295	1533	3104	2745	109.22
14	58,000		2.0	7684	713	1086	166	1539	1806	1424	56.99
13			2.0	7698	709	1086	167	1545	1841	1474	58.12
12			2.0	7670	708	1094	167	1565	1657	1495	58.02
16	70,000		2.0	7698	708	612	170	1583	880	774	31.89

aPrimary uniform

bBoth sector

LARGE BURNER

Engine fuel flow, $w_{f,e}$, lb/hr	After- burner fuel flow, $w_{f,ab}$, lb/hr	Tail- rake gas flow, $w_{g,s}$, lb/sec	Afterburner fuel-air ratio based on unburned air, f_{ua}	Jet thrust, F_j , lb	Calculated afterburner total temperature, $T_{n,cr}$	Exhaust- nozzle, diameter, D_n , in.	Afterburner combustion efficiency, η_{ab}	Burner total- pressure loss ratio, $P_s - P_g$ P_s	Diffuser- inlet Mach number, M_5	Burner total- temperature ratio, T_p/T_5
two-V-flameholder										
4510	16,750	93.80	0.0671	11,313	3741	29.20	0.787	0.110	0.51	2.515
4560	16,910	94.87	0.0669	11,409	3691	29.07	.769	.106	.51	2.484
4670	16,960	96.52	0.0661	11,751	3717	29.00	.790	.105	.51	2.472
4690	15,310	96.20	0.0596	11,586	3620	28.68	.827	.101	.51	2.408
4700	13,970	95.77	0.0546	11,421	3514	28.28	.845	.097	.51	2.323
4700	11,960	94.97	0.0469	11,047	3335	27.69	.882	.092	.51	2.203
4680	10,780	94.34	0.0425	10,712	3171	27.23	.871	.088	.51	2.096
4660	9,525	94.30	0.0374	10,334	2945	26.65	.839	.085	.51	1.980
4660	8,620	93.88	0.0339	9,987	2774	26.11	.805	.079	.51	1.856
4560	8,7825	92.24	0.0315	9,521	2637	25.80	.789	.076	.51	1.774
4445	7,760	92.02	0.0309	9,516	2617	25.70	.784	.076	.51	1.756
4690	7,705	94.59	0.0301	9,535	2489	25.43	.684	.074	.52	1.653
4955	13,500	117.11	0.0504	14,423	3208	28.63	.877	.122	.57	2.068
1535	5,990	31.19	0.0729	3,560	3439	28.79	.604	.095	.53	2.274
1460	45,055	29.65	0.0443	3,338	3427	28.70	.677	.102	.53	2.248
2635	9,040	62.15	0.0524	7,884	3614	29.70	.878	.124	.56	2.324
2645	7,860	61.73	0.0457	7,577	3364	29.04	.863	.119	.56	2.169
2645	6,155	62.09	0.0553	7,053	2860	27.77	.767	.105	.58	1.846
1440	4,850	34.03	0.0512	3,822	3407	29.60	.791	.132	.58	2.186
1470	4,100	34.00	0.0434	3,651	3035	28.74	.720	.123	.59	1.952
antislowl vanes installed										
4720	16,925	93.42	0.0692	11,684	3797	28.47	0.785	0.099	0.50	2.399
4735	15,400	93.28	0.0627	11,672	3751	28.34	.843	.100	.51	2.387
4700	13,650	93.08	0.0552	11,433	3592	28.10	.866	.100	.51	2.286
4700	11,905	92.33	0.0484	11,145	3428	27.65	.896	.093	.51	2.168
4700	10,215	91.98	0.0415	10,944	3195	26.98	.893	.087	.51	2.044
4680	8,535	91.59	0.0346	10,138	2938	26.28	.861	.081	.51	1.876
4680	6,855	91.06	0.0276	9,432	2561	25.11	.772	.073	.51	1.631
5100	15,315	118.39	0.0475	14,952	3517	29.66	.915	.131	.58	2.245
5000	13,970	115.21	0.0437	14,577	3380	29.22	.911	.127	.58	2.178
vanes installed; new spray-bar spacing										
4385	16,955	92.14	0.0691	10,968	3596	28.96	0.696	0.107	0.53	2.362
4385	15,370	91.77	0.0628	10,912	3562	28.83	.755	.108	.53	2.345
4375	13,700	91.05	0.0560	10,702	3466	28.51	.797	.105	.53	2.291
4395	11,950	90.36	0.0491	10,483	3367	28.06	.854	.100	.53	2.223
4370	10,225	89.99	0.0419	10,106	3093	27.35	.830	.094	.53	2.052
4350	8,770	89.60	0.0359	9,640	2852	26.55	.803	.086	.53	1.890
4385	6,835	89.33	0.0279	8,398	2186	24.41	.485	.070	.52	1.434
4890	10,730	111.22	0.0344	13,159	2901	28.38	.821	.116	.59	1.892
2450	5,815	56.09	0.0356	6,616	2735	28.38	.664	.113	.60	1.777
2335	5,195	59.05	0.0314	6,372	2431	26.93	.580	.102	.60	1.573
2515	5,195	58.94	0.0312	6,281	2382	27.03	.507	.098	.59	1.509
1415	3,350	32.54	0.0367	3,319	2653	28.46	.599	.120	.63	1.676

4644

CI-4

TABLE II. - Concluded.

Run	Altitude, ft	Flight Mach number, M ₀ , nominal	Variable stator position, deg from open position	Engine speed, N, rpm	Compressor- inlet total temperature, T ₂ , °R	Compressor- inlet total pressure, P ₂ , lb sq ft abs	Tank ambient pressure, P _{tank} , lb sq ft abs	Diffuser- inlet total temperature, T ₅ , °R	Diffuser- inlet total pressure, P ₅ , lb sq ft abs	Tailrake total pressure, P _g , lb sq ft abs	Compressor- inlet airflow, lb/sec
(d) Configuration 8 ₁											
6	35,000	1.16	0	7461	500	1147	502	1542	2683	2594	90.92
5			0	7461	500	1146	494	1541	2650	2570	90.92
4			0	7459	500	1144	494	1537	2680	2613	90.77
3			0	7464	500	1144	501	1537	2669	2619	90.77
2			0	7459	499	1153	489	1529	2659	2629	91.31
1			0	7458	502	1147	493	1532	2686	2673	90.48
12			1	7485	510	1139	493	1523	-----	2369	89.82
13			1	7489	510	1140	497	1509	-----	2376	89.92
11			1	7483	512	1142	512	1513	-----	2394	89.86
10			1	7486	515	1137	505	1515	-----	2405	88.97
15			0	7458	507	1145	490	1509	2693	2413	90.90
9			0	7470	501	1131	492	1493	2681	2325	90.91
10			0	7464	502	1142	483	1502	2688	2333	91.38
8			0	7462	503	1144	492	1496	2670	2319	91.34
7			0	7459	504	1155	499	1499	2701	2355	90.85
14			1	7491	509	1138	505	1501	-----	2442	89.85
9			1	7483	518	1143	505	1505	-----	2412	88.45
15			1	7490	508	1136	499	1502	-----	2476	89.95
14			0	7485	505	1139	504	1460	2595	2251	90.79
13			0	7466	504	1150	497	1437	2600	2252	91.40
12			0	7461	504	1132	491	1466	2578	2242	90.79
11			0	7459	504	1148	474	1465	2607	2276	91.10
16			0	7484	508	1145	502	1463	2596	2310	90.88
5			1	7471	510	1141	501	1519	-----	2445	89.86
8			1	7478	509	1136	486	1615	-----	2554	89.87
7			1	7472	506	1141	515	1614	-----	2476	90.34
8			1	7477	505	1139	499	1521	-----	2499	90.70
4			1	7475	514	1141	492	1513	-----	2494	89.34
8	45,000		1/2	7478	501	704	315	1516	1674	1460	56.12
9			1/2	7475	501	710	308	1514	1677	1465	58.55
7			1/2	7484	502	704	306	1517	1669	1472	55.98
6			1/2	7473	502	712	287	1525	1660	1480	56.46
5			1/2	7474	503	709	313	1521	1662	1492	56.26
4			1/2	7474	503	704	316	1618	1665	1494	56.00
3			1/2	7474	505	709	311	1519	1668	1499	56.09
2			1/2	7474	508	710	325	1519	1667	1506	55.85
22		2.00	2	7726	706	2037	329	1545	3240	2833	111.72
23			2	7733	700	2031	317	1544	3223	2830	111.90
21			2	7727	706	2042	318	1547	3245	2869	111.82
24			2	7722	700	2032	302	1548	3232	2870	111.62
20			2	7726	707	2046	297	1552	3247	2896	111.73
25			2	7730	700	2042	293	1546	3264	2927	112.47
19			2	7732	708	2050	306	1546	3245	2916	111.55
9	55,000	1.16	1/2	7476	502	434	134	1514	993	856	34.23
8			1/2	7462	503	435	120	1519	989	867	34.25
7			1/2	7464	503	433	124	1510	997	874	34.10
6			1/2	7458	503	433	136	1516	982	871	34.39
10			1/2	7479	502	431	137	1510	989	882	34.14
4			1/2	7446	507	432	128	1513	996	887	35.84
3			1/2	7451	509	431	132	1516	993	889	35.78
2			1/2	7449	510	430	132	1523	989	893	35.58
5			1/2	7451	500	431	145	1521	990	904	34.20
11		2.00	1	7745	703	1173	174	1525	1811	1558	66.69
12			1/2	7751	703	1165	148	1511	1806	1544	66.32
13	58,000		2	7704	707	1089	187	1567	1717	1501	58.75
12			2	7704	708	1096	188	1564	1721	1508	58.81
11			2	7708	708	1086	176	1554	1701	1491	58.69
10			2	7711	708	1080	179	1554	1694	1491	58.69
9			2	7714	711	1088	175	1557	1695	1500	58.34
15	70,000		2 1/4	7674	704	615	156	1562	931	831	32.25
16			2 1/4	7684	704	615	190	1590	935	820	32.25
17			2 1/4	7665	705	615	190	1578	930	818	31.97

LARGE BURNER

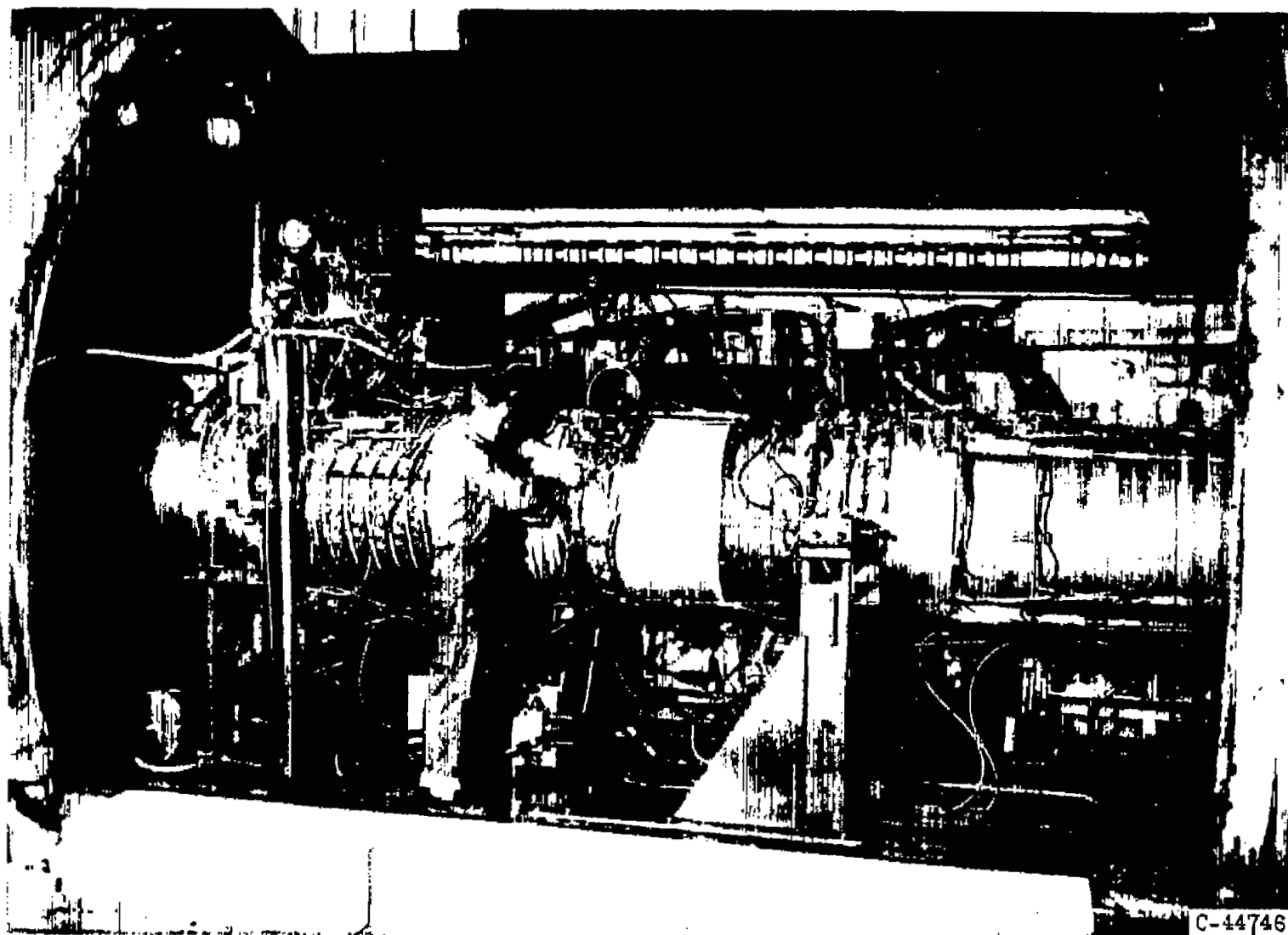
Engine fuel flow, $W_{f,e}$, lb/hr	After- burner fuel flow, $W_{f,ab}$, lb/hr	Tail- rake gas flow, $W_{g,9}$, lb/sec	Afterburner fuel-air ratio based on unburned air, F_{ua}	Jet thrust, F_j , lb	Calculated afterburner total temperature, T_{tr} , °R	Exhaust- nozzle, total diameter, D_n , in.	Afterburner combustion efficiency, η_{ab}	Burner total- pressure loss ratio, $P_5 - P_9$	Diffuser- inlet Mach number, M_5	Burner total- temperature ratio, T_9/T_5
three-V-flameholder										
4745	16,905	95.02	0.0675	11,933	3635	28.74	0.826	0.100	0.50	2.486
4735	15,000	94.49	0.0600	11,664	3683	28.41	.851	.098	.51	2.590
4735	13,430	93.91	0.0538	11,599	3661	28.18	.936	.093	.50	2.582
4735	11,680	93.42	0.0468	11,117	3408	27.83	.920	.087	.50	2.216
4735	9,910	93.46	0.0395	10,737	3143	27.02	.913	.081	.51	2.056
4735	8,195	92.17	0.0333	10,040	2818	26.07	.840	.074	.50	1.839
4680	15,955	93.30	0.0649	11,434	3783	29.61	.833	-----	-----	2.484
4660	14,320	92.94	0.0591	11,242	3688	29.31	.881	-----	-----	2.443
4650	12,655	92.22	0.0517	10,817	3475	28.75	.867	-----	-----	2.296
4610	10,900	91.06	0.0450	10,450	3287	28.09	.884	-----	-----	2.169
4640	8,885	92.36	0.0357	10,056	2910	27.00	.852	.104	.54	1.926
4630	13,980	93.81	0.0559	11,205	3614	29.41	.880	.133	.54	2.421
4620	13,970	94.26	0.0555	11,256	3643	29.75	.901	.132	.55	2.425
4600	13,630	94.12	0.0541	11,168	3569	29.24	.884	.132	.56	2.585
4650	13,460	93.59	0.0540	11,203	3622	29.01	.913	.128	.54	2.416
4670	9,250	91.47	0.0381	10,203	3080	27.25	.910	-----	-----	2.052
4580	9,120	90.05	0.0381	9,922	3008	27.32	.858	-----	-----	1.998
4690	7,540	91.09	0.0315	9,500	2683	26.15	.786	-----	-----	1.773
4445	12,600	93.26	0.0500	10,695	3459	29.77	.898	.133	.56	2.568
4465	12,600	93.86	0.0498	10,796	3426	29.52	.889	.134	.59	2.584
4445	12,575	93.19	0.0491	10,660	3357	29.24	.859	.130	.57	2.289
4495	11,995	93.40	0.0476	10,776	3357	28.98	.876	.127	.56	2.277
4455	8,270	92.15	0.0331	9,525	2700	27.00	.781	.110	.56	1.846
4650	13,630	92.69	0.0555	10,064	2907	27.31	.544	-----	-----	1.913
4670	11,825	92.20	0.0483	10,164	2952	27.13	.649	-----	-----	1.948
4670	10,250	92.22	0.0416	9,949	2883	26.80	.711	-----	-----	1.904
4700	8,030	91.97	0.0327	9,657	2688	26.12	.764	-----	-----	1.767
4630	5,610	89.96	0.0236	6,874	2357	25.12	.737	-----	-----	1.558
2935	9,600	58.20	0.0626	6,929	3665	29.82	.809	.128	.54	2.417
2925	8,920	58.43	0.0576	6,926	3560	29.41	.824	.126	.54	2.352
2916	7,555	57.49	0.0495	6,652	3343	28.57	.836	.118	.54	2.203
2918	6,155	57.57	0.0400	6,435	3013	27.65	.824	.108	.55	1.976
2905	9,600	58.32	0.0621	5,924	2564	26.86	.356	.102	.55	1.686
2905	7,430	57.47	0.0487	6,175	2885	27.31	.610	.103	.54	1.699
2905	5,850	57.12	0.0383	6,055	2788	26.89	.713	.101	.54	1.836
2905	4,425	56.49	0.0294	5,727	2588	26.13	.768	.097	.54	1.703
4920	14,225	114.69	0.0446	14,635	3476	29.45	.951	.126	.57	2.248
4920	13,330	114.62	0.0418	14,575	3309	29.05	.913	.122	.56	2.143
4930	12,620	114.35	0.0396	14,235	3241	28.83	.918	.116	.57	2.094
4920	11,785	113.92	0.0370	13,988	3117	28.29	.899	.112	.57	2.013
4930	10,990	113.80	0.0346	13,748	2998	28.06	.878	.108	.57	1.932
4950	10,090	114.29	0.0316	13,468	2831	27.58	.841	.103	.57	1.831
4910	9,375	113.18	0.0296	13,084	2747	27.26	.829	.101	.57	1.777
1775	5,840	35.49	0.0623	4,297	3379	-----	.681	.138	.56	2.232
1775	5,495	35.41	0.0586	4,339	3283	-----	.677	.132	.56	2.162
1775	4,665	35.04	0.0501	4,125	3112	-----	.708	.123	.55	2.061
1765	3,770	35.07	0.0401	3,894	2776	-----	.675	.113	.58	1.831
1765	3,100	34.64	0.0335	3,504	2294	-----	.481	.106	.57	1.520
1755	4,125	34.82	0.0448	3,856	2725	27.31	.577	.109	.55	1.801
1775	3,445	34.38	0.0378	3,777	2673	27.09	.652	.105	.55	1.761
1745	2,775	33.99	0.0306	3,620	2509	26.38	.679	.097	.55	1.648
1765	2,125	34.43	0.0229	3,139	1887	-----	.317	.087	.57	1.241
2650	9,090	68.37	0.0490	7,619	3089	29.87	.683	.141	.63	2.006
2925	7,930	67.68	0.0422	8,039	2894	29.35	.667	.145	.63	1.889
2625	8,565	60.57	0.0493	7,666	3510	29.72	.864	.126	.57	2.238
2625	8,255	60.59	0.0494	7,662	3467	29.48	.855	.124	.57	2.262
2600	7,520	60.27	0.0449	7,376	3203	29.29	.787	.124	.58	2.062
2575	6,855	60.08	0.0408	7,312	3158	28.92	.837	.120	.58	2.032
2565	6,195	57.55	0.0374	7,021	2933	28.46	.767	.115	.57	1.883
1460	4,955	33.35	0.0535	3,884	3342	29.72	.719	.127	.59	2.113
1460	4,475	33.22	0.0487	3,625	3132	29.19	.682	.123	.59	1.970
1430	3,755	32.74	0.0412	3,461	2921	28.51	.685	.120	.58	1.851

4644

CI-4 back

TABLE III. - AFTERBURNER CONFIGURATIONS

Configuration	Diffuser		Flameholder				Fuel bars		Sketch of configuration in figure	Outer-shell nominal diameter, in.
	Vortex generators	Swirl vanes	Designation	Type	Position, in. from spray bars	Blockage, percent	Designation	Number and type		
1	Yes	No	A	Three-V-gutter	11.4	37	A	40 Individual	5	33.7
2	No	No	B	Two-V-gutter	9.5	30	B	20 Tandem		33.7
3	No	No	C	Three-V-gutter	11.4	30	B	20 Tandem		33.7
4	No	No	C	Three-V-gutter	16.4	30	B	20 Tandem		33.7
5	Yes	No	D	Two-V-gutter	11.75	30	C	20 Tandem		35.7
6	Yes	Yes	D	Two-V-gutter	11.75	30	C	20 Tandem		35.7
7	Yes	Yes	D	Two-V-gutter	11.75	30	D	20 Tandem		35.7
8	Yes	No	E	Three-V-gutter	13.0	30	C	20 Tandem		35.7
9	Yes	No	F	Three-V-gutter	13.0	30	C	20 Tandem	6	33.7



C-44746

Figure 1. - The XJ79 installation in the altitude test chamber.

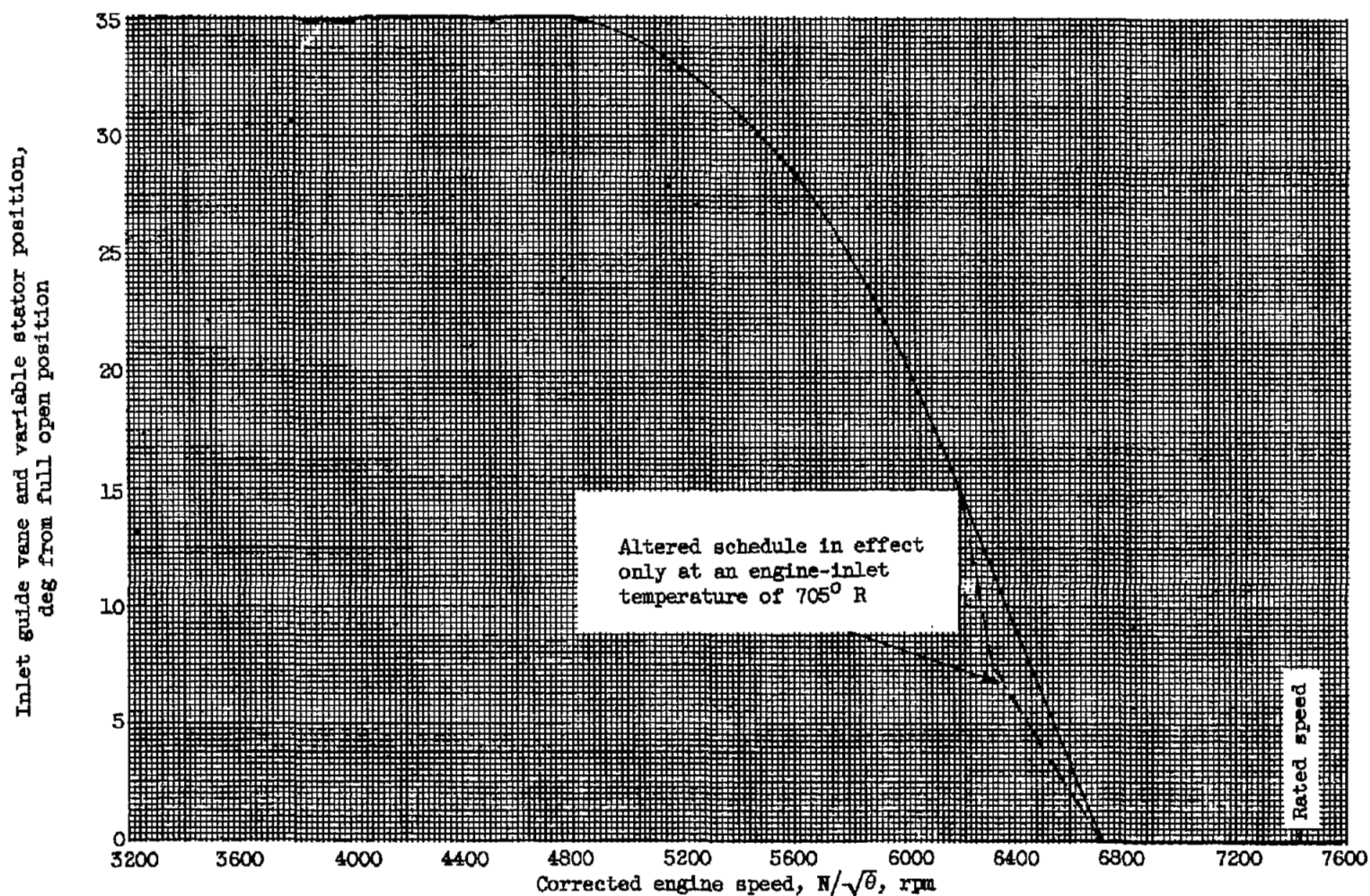


Figure 2. - The variation of inlet-guide vane and variable stator position with corrected engine speed for the original schedule and for the reset schedule in effect at an engine-inlet temperature of 705° R.

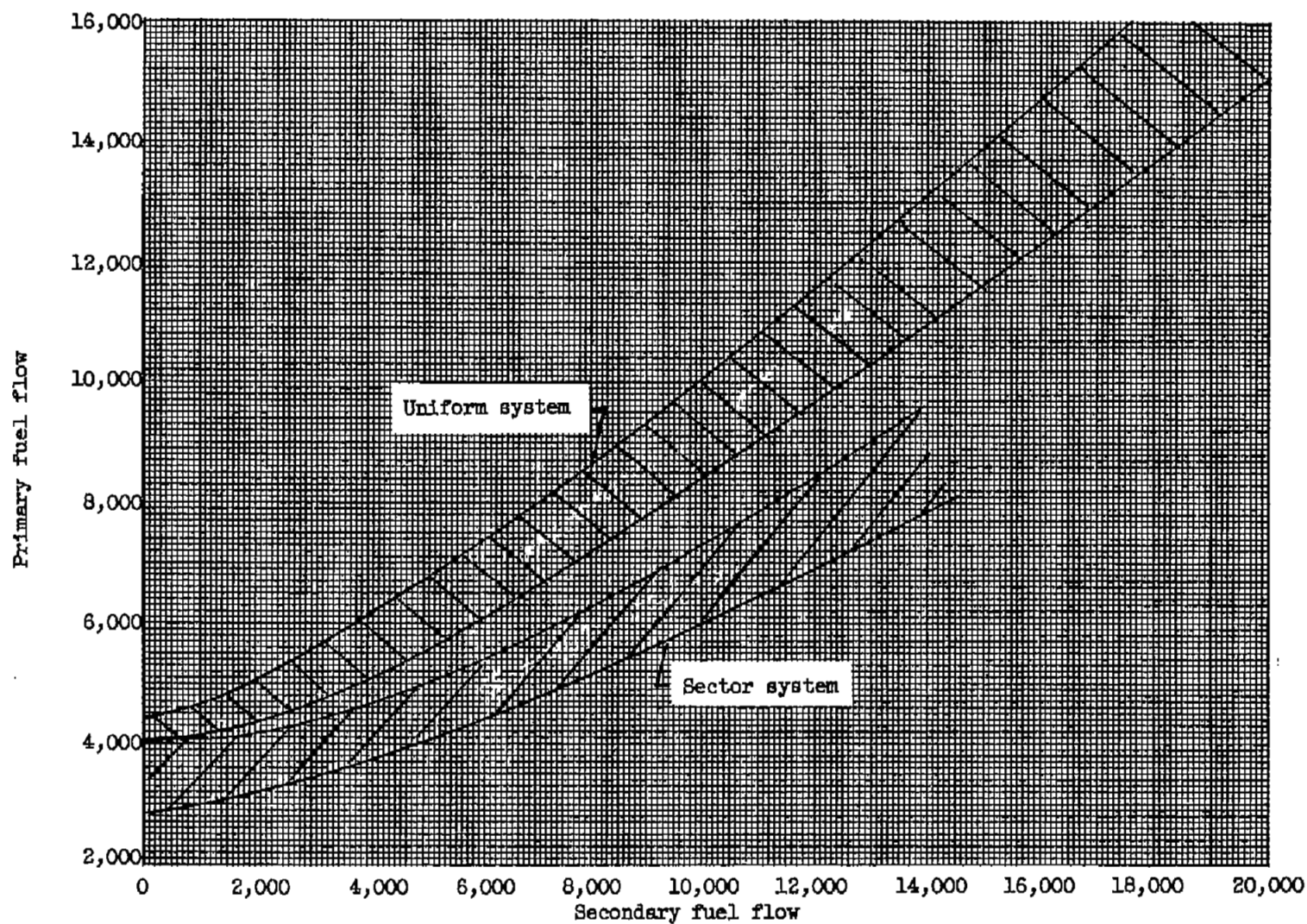
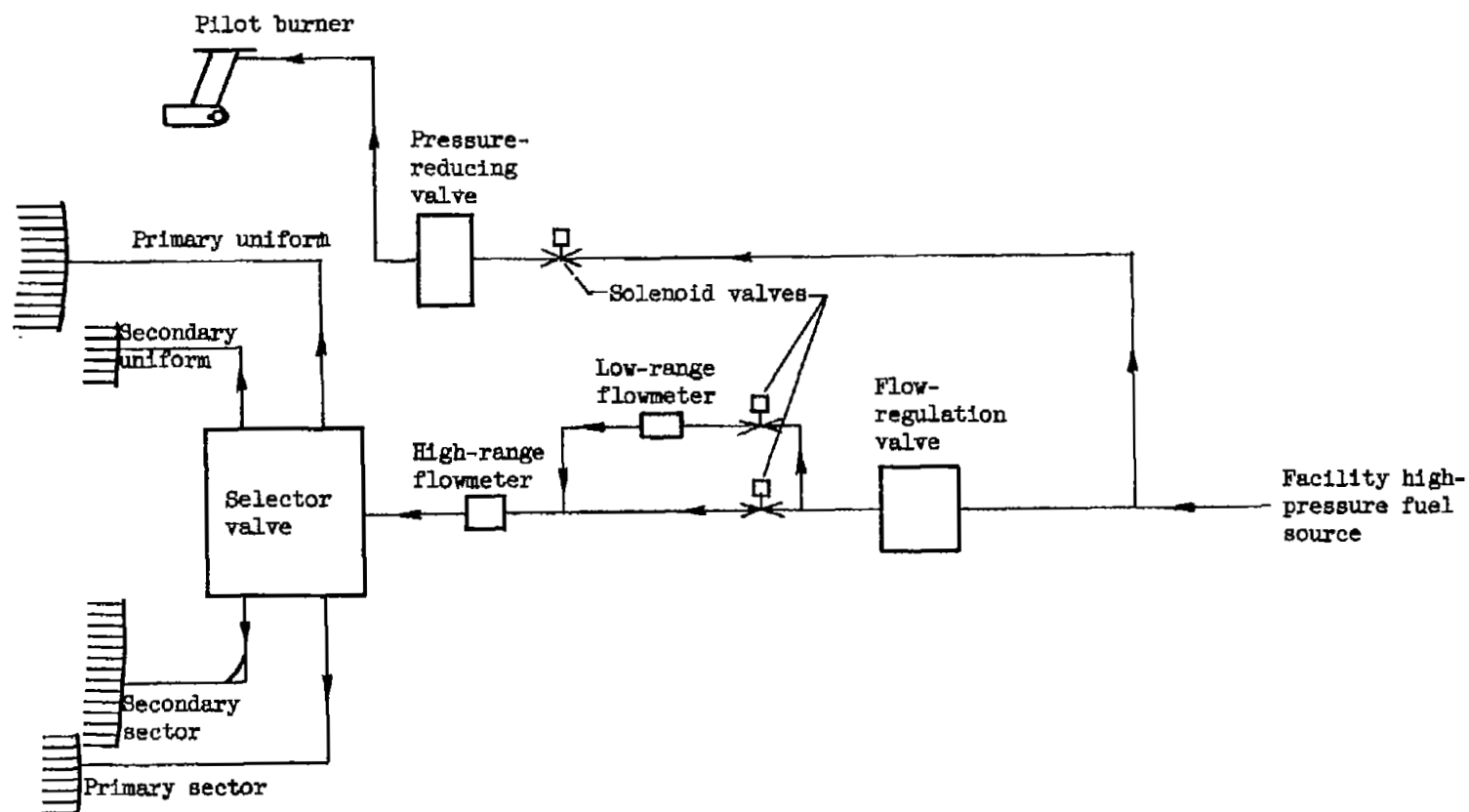


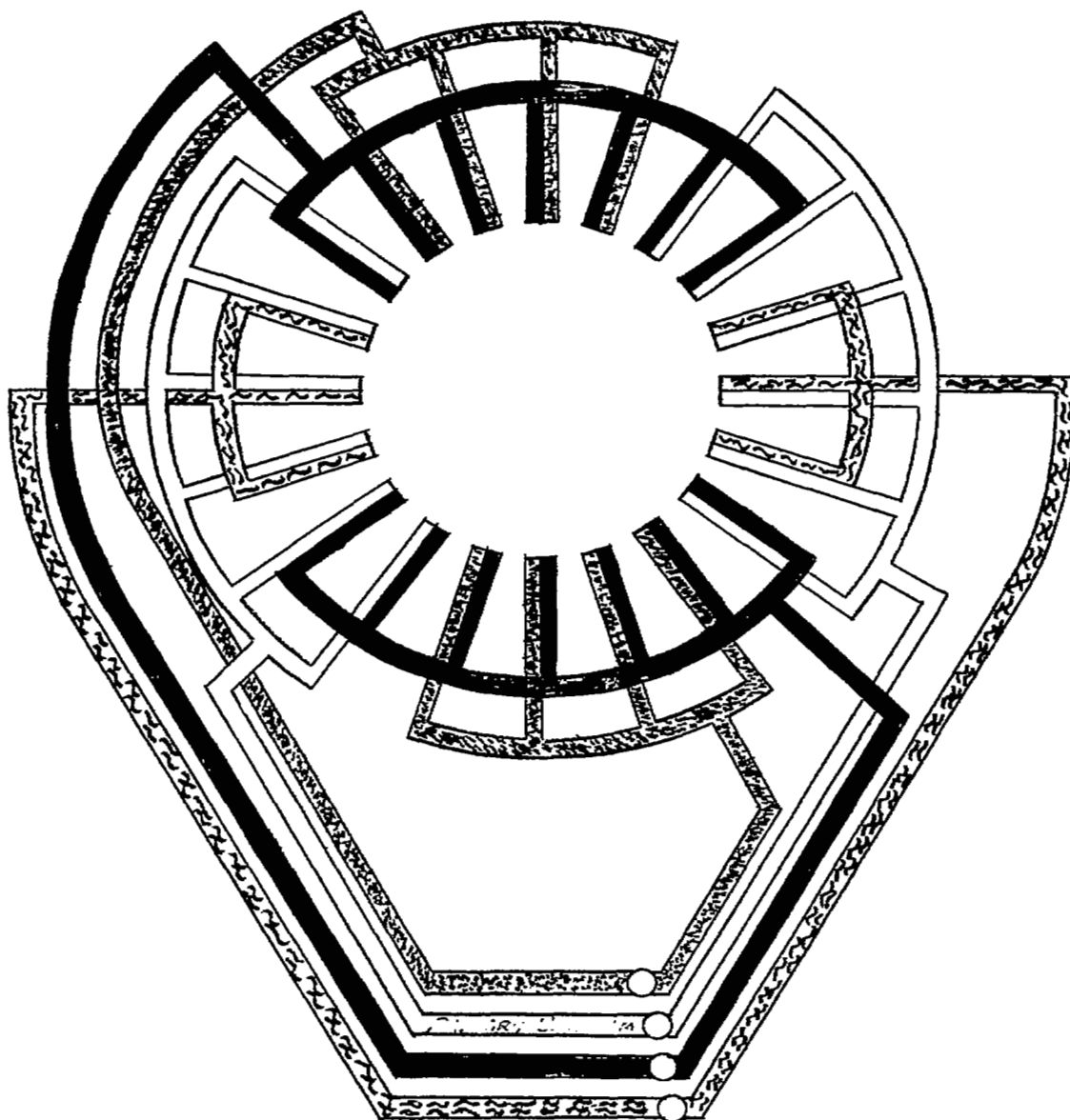
Figure 3. - The relation between amounts of fuel provided in the primary and secondary fuel systems during sector and uniform burning by the selector valve.



(a) Fuel system used during investigation.

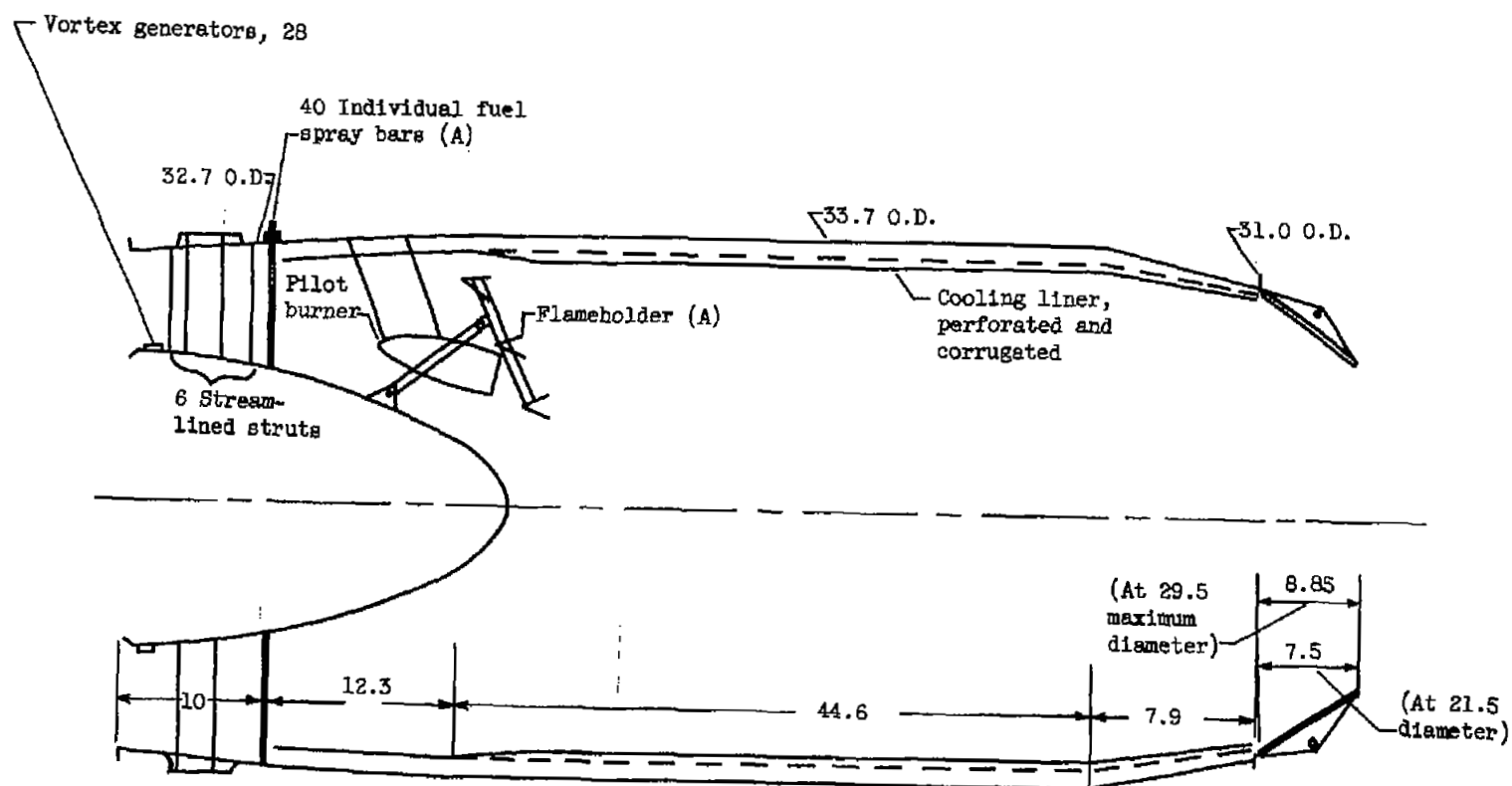
Figure 4. - Schematic drawing of afterburner.

Solid	Secondary sector
Open	Primary uniform
≈≈≈	Secondary uniform
~~~~~	Primary sector



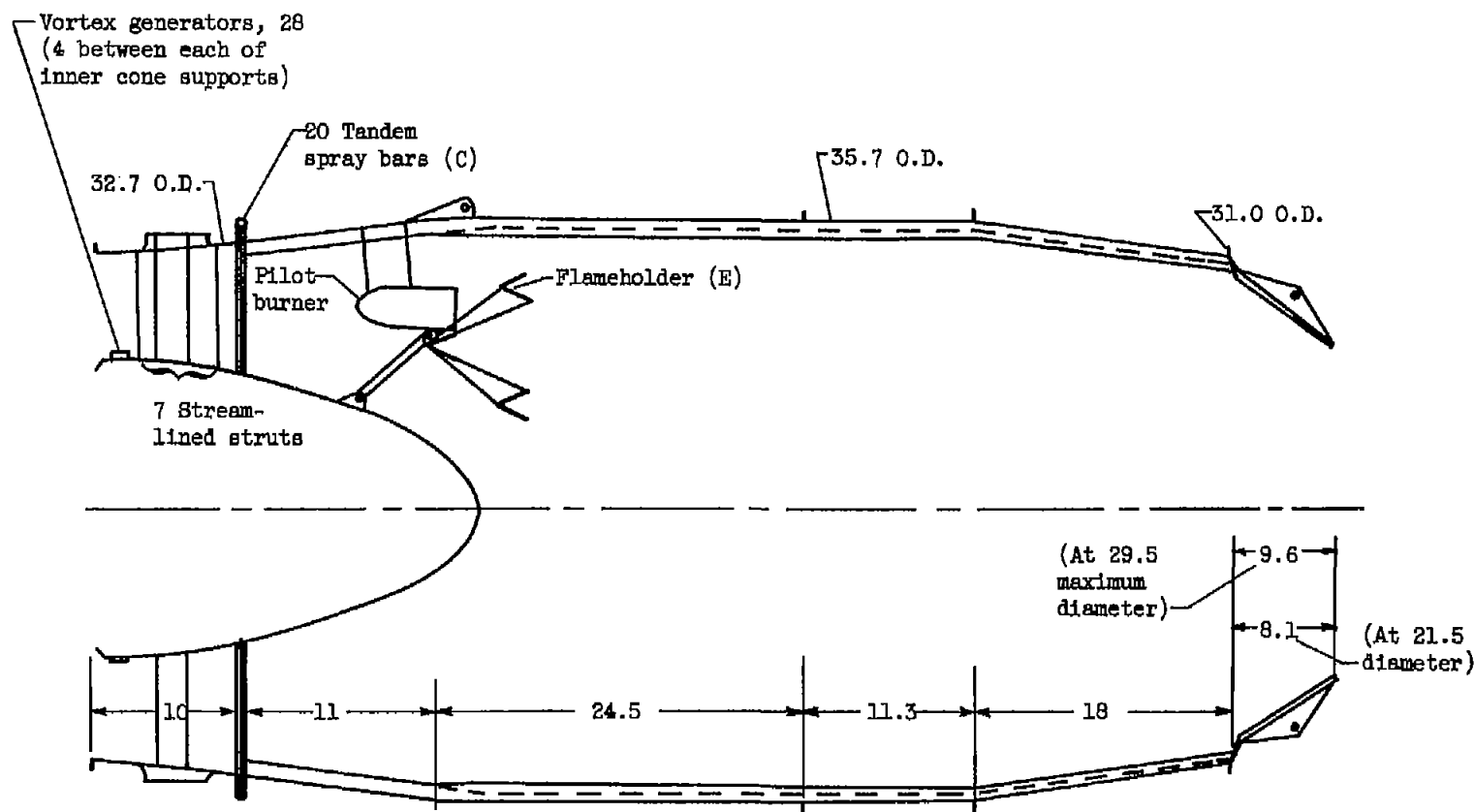
(b) Tandem fuel-spray-bar manifold showing top and bottom sections providing fuel during sector burning.

Figure 4. - Concluded. Schematic drawing of afterburner.



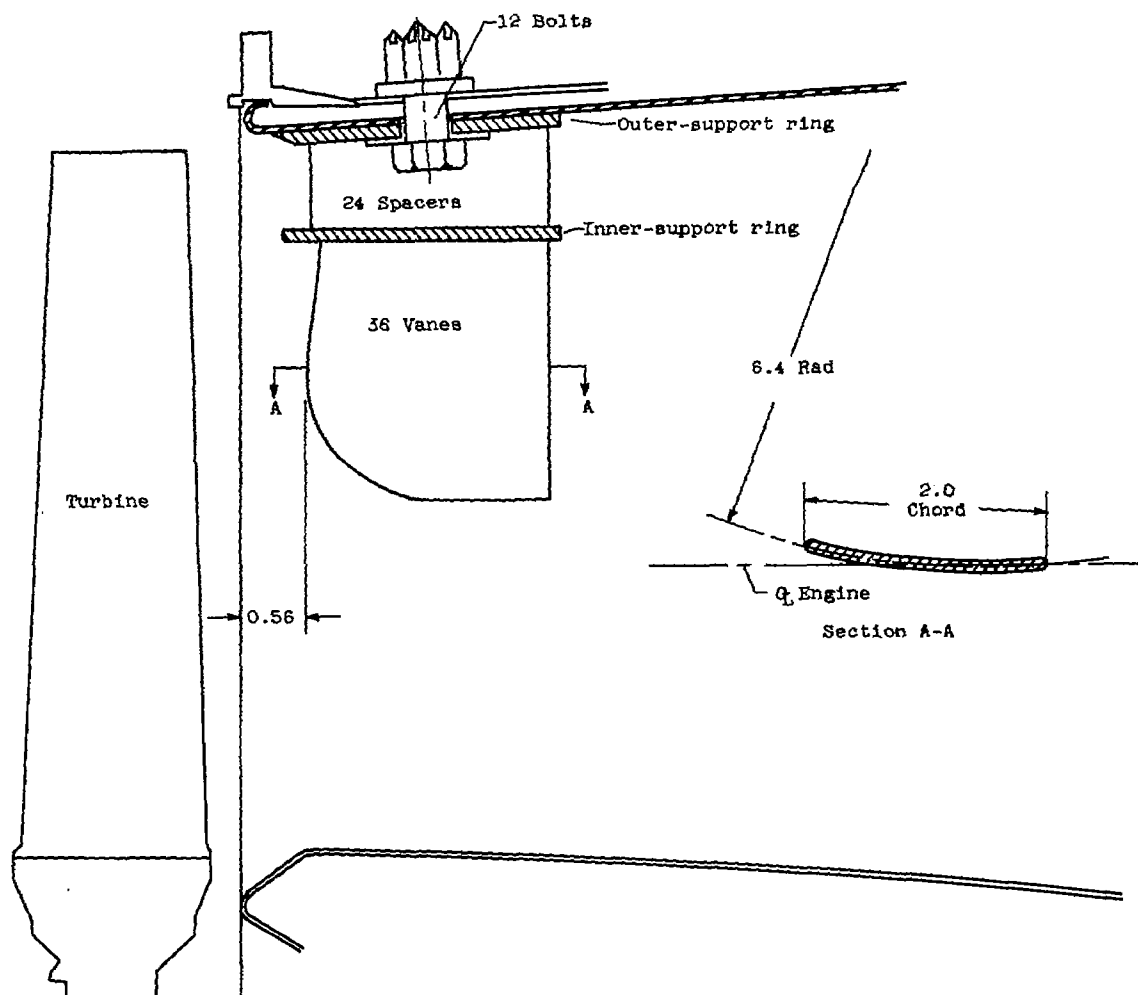
(a) Configuration 1.

Figure 5. - Burner details. (All dimensions in inches.)



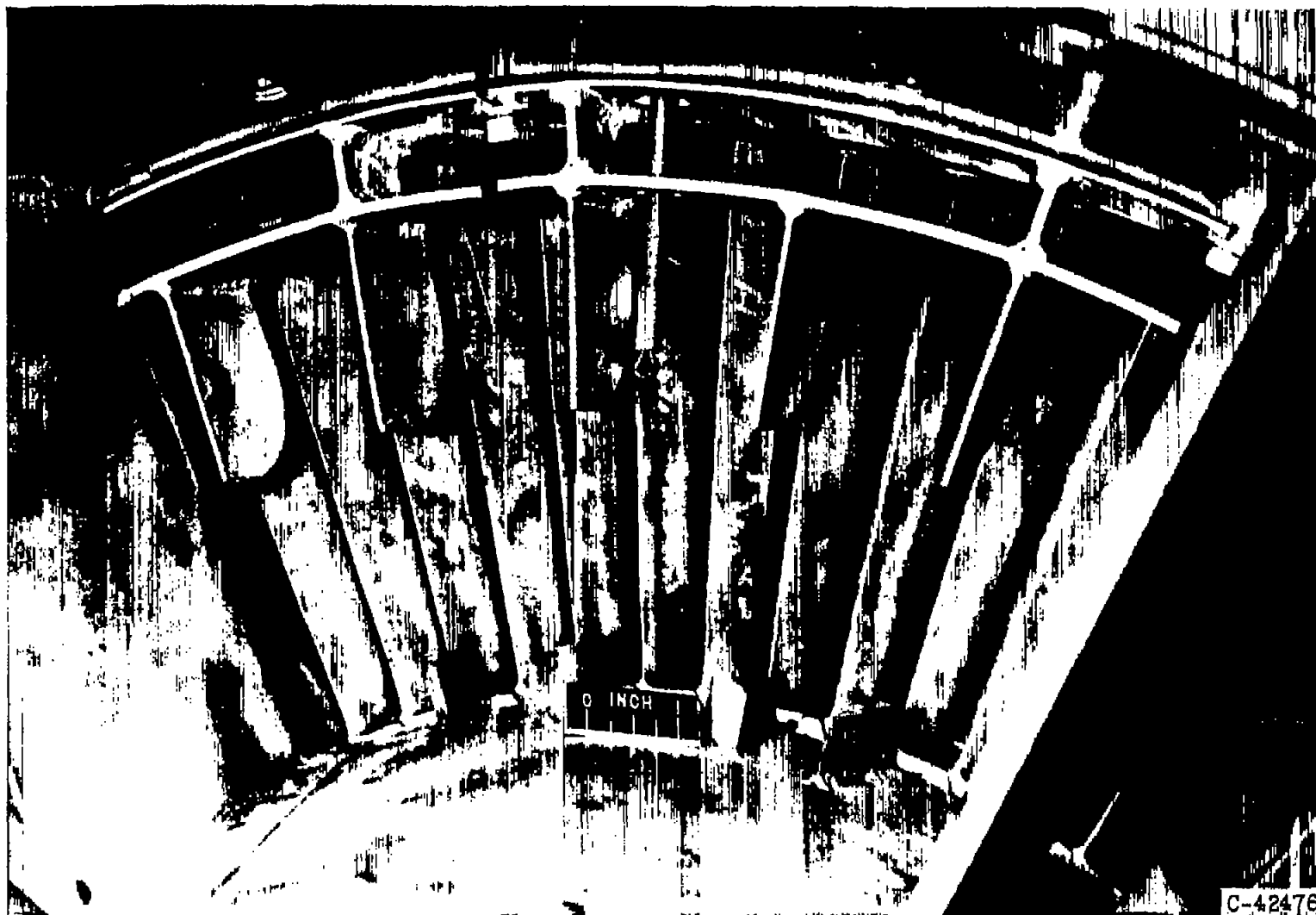
(b) Configuration 8

Figure 5. - Concluded. Burner details. (All dimensions in inches.)



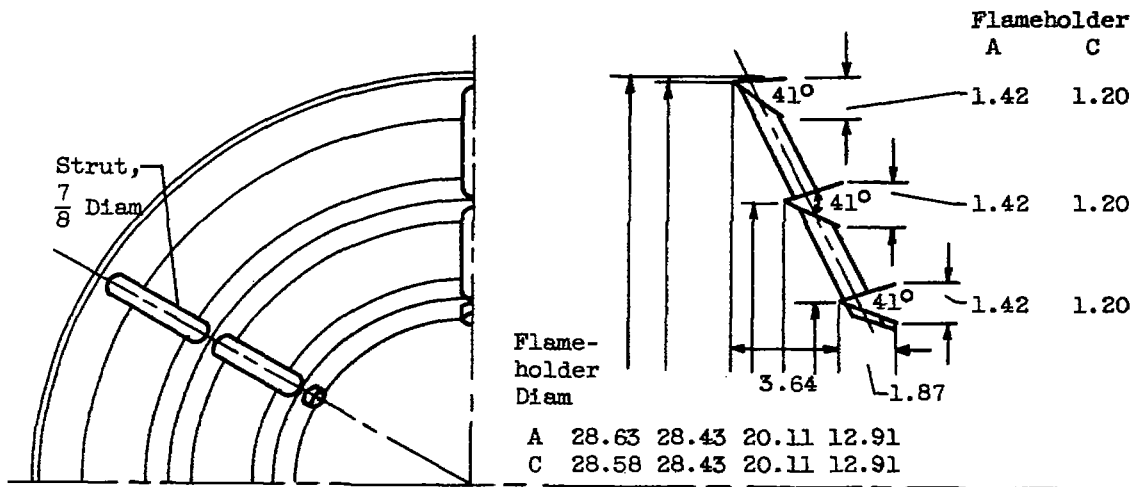
(a) Schematic drawing of vanes.

Figure 6. - Turbine-outlet section showing installation of 36 equally spaced antiwhirl vanes.  
(All dimensions in inches.)

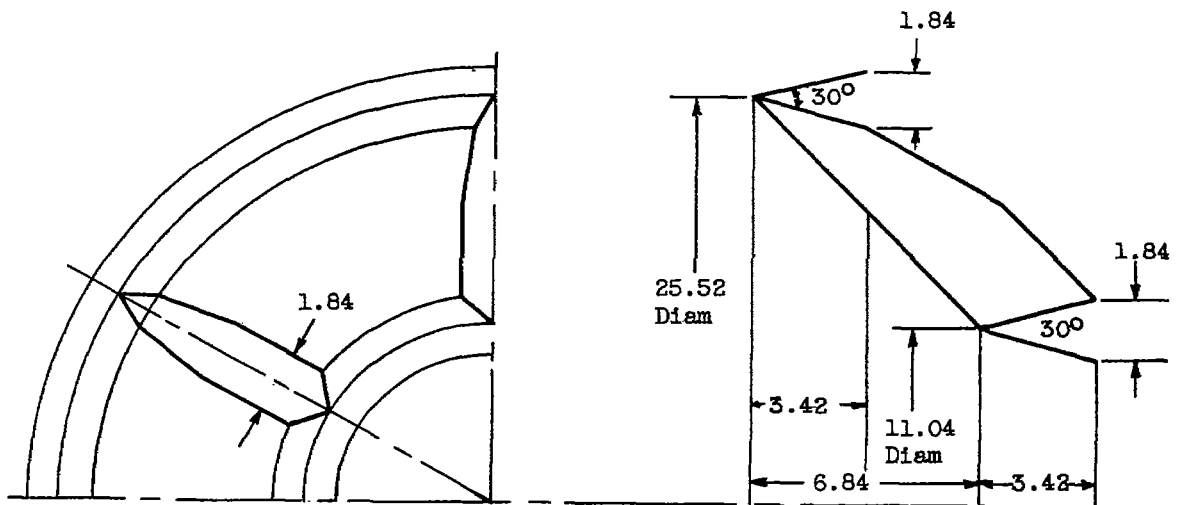


(b) Photograph of vanes and vortex generators.

Figure 6. - Concluded. Turbine-outlet section showing installation of 36 equally spaced antiwhirl vanes.

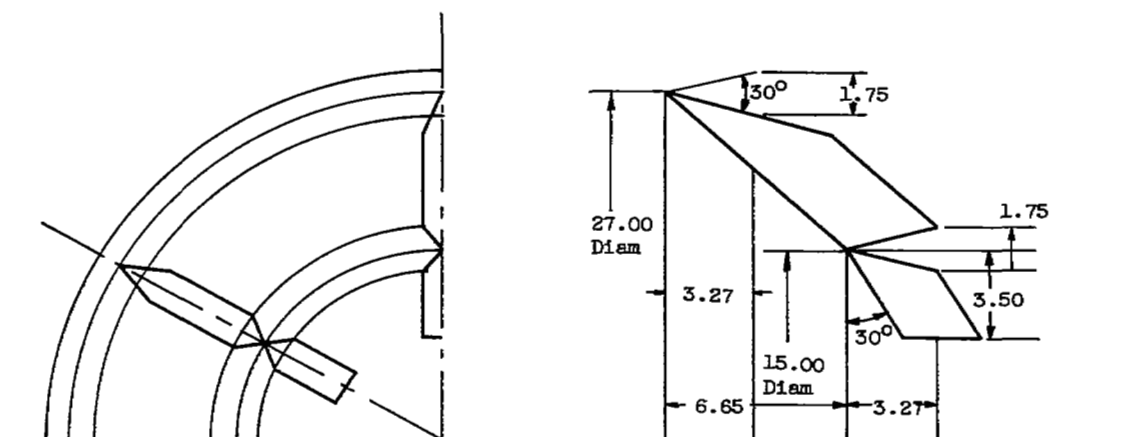


(a) Flameholder projected area of designations A and B, 313.5 and 253.5 square inches, respectively.

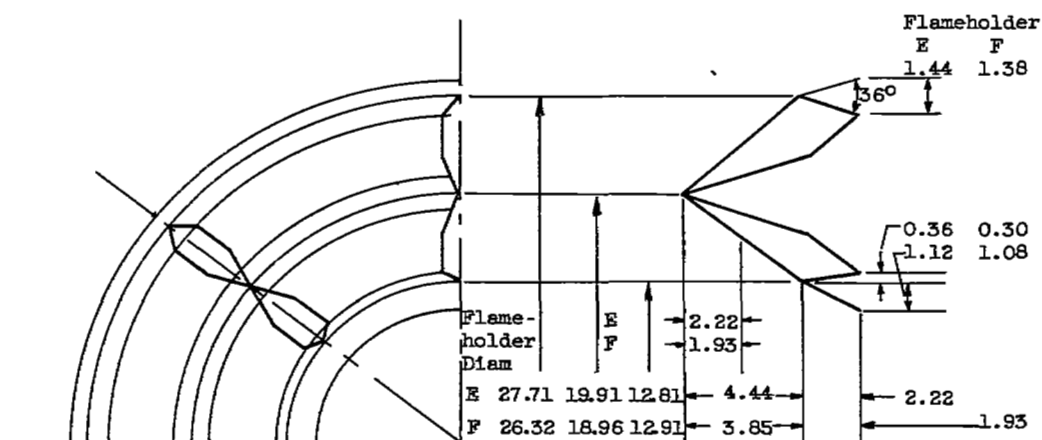


(b) Flameholder projected area of designation B, 270.6 square inches.

Figure 7. - Schematic diagrams of flameholders. (All dimensions are in inches.)



(c) Flameholder projected area of designation D, 291.7 square inches.



(d) Flameholder projected area of designations E and F, 304 and 284 square inches, respectively.

Figure 7. - Concluded. Schematic diagrams of flameholders. (All dimensions are in inches.)

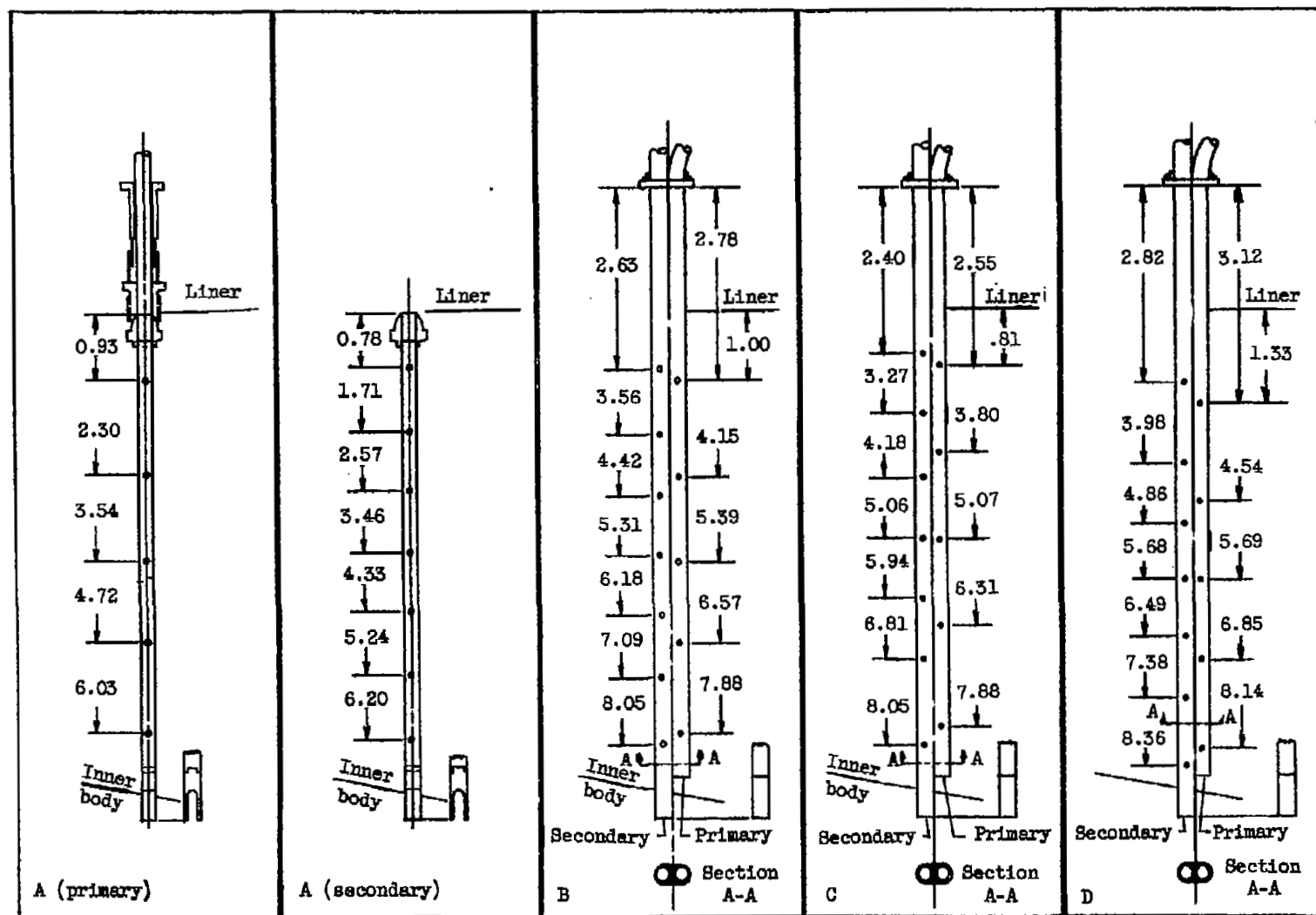
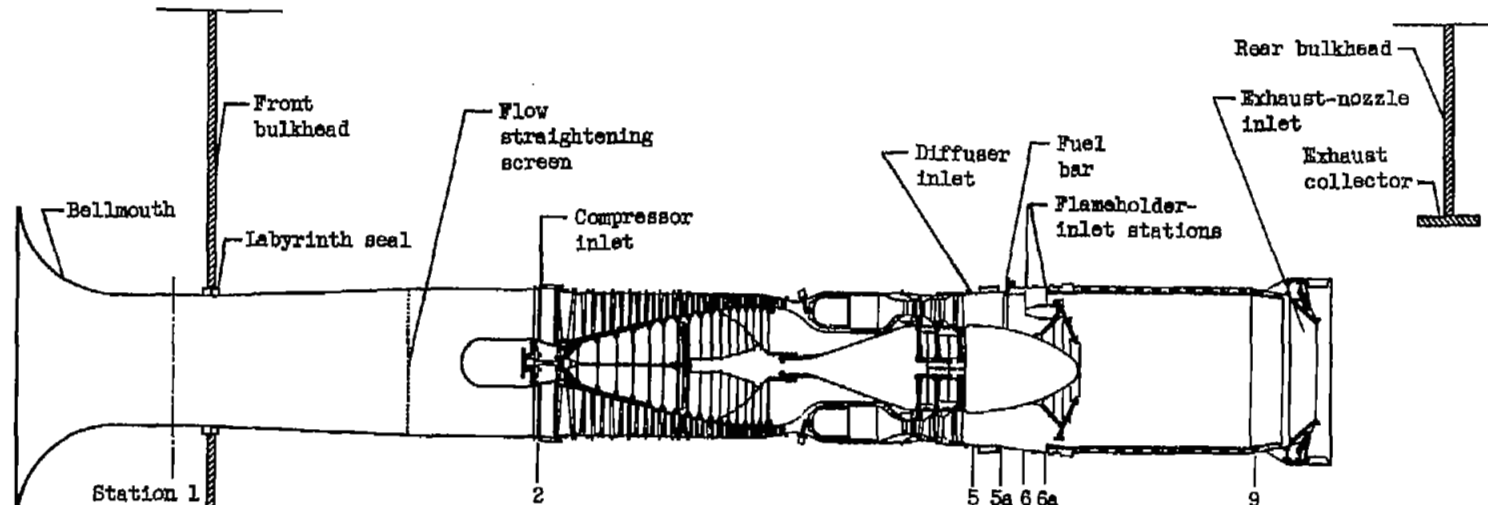


Figure 8. - Details of afterburner fuel spray bars. Tubes, 0.250 O.D.X0.035 wall; orifices, 0.028 diameter through both sides. (All dimensions in inches.)



	Station	Number of probes			Number of rakes
		Total pressure	Wall static pressure	Thermocouple	
Airflow measuring	1	24	4	8	4
Engine inlet	2	9	0	9	1
Diffuser inlet	5	30	2	39	6
Fuel bar	5a	10	2	5	0
Flameholder inlet	6 (6a)	11	2	0	1
Exhaust-nozzle inlet	9	13	1	0	1
Tank ambient	0	4	trailing static probes		

CD-5459

Figure 9. - Schematic diagram of engine and instrumentation stations.

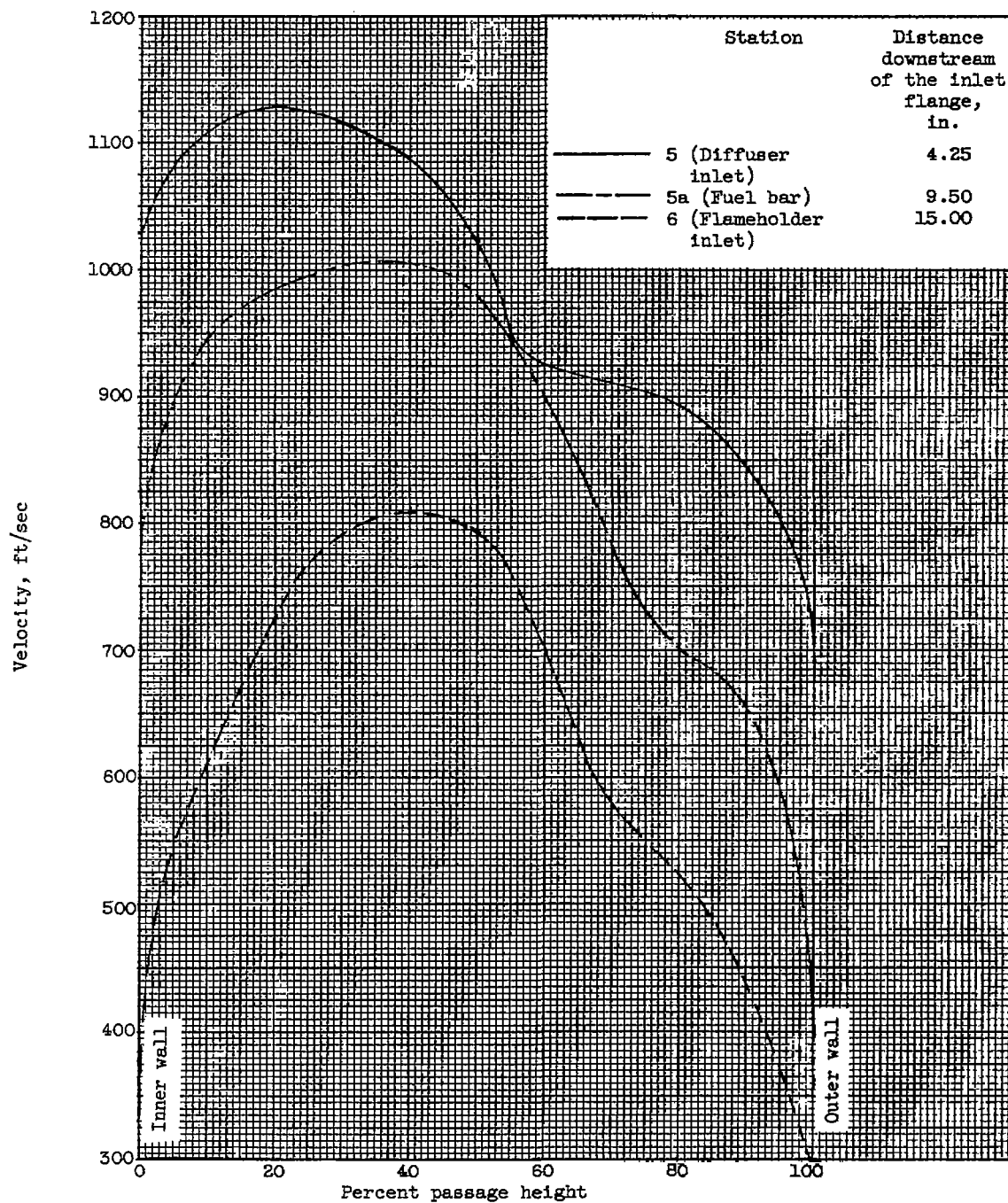


Figure 10. - Velocity profiles through the diffuser of the original configuration (1) at a flight condition of 35,000 feet and a Mach number of 1.16.

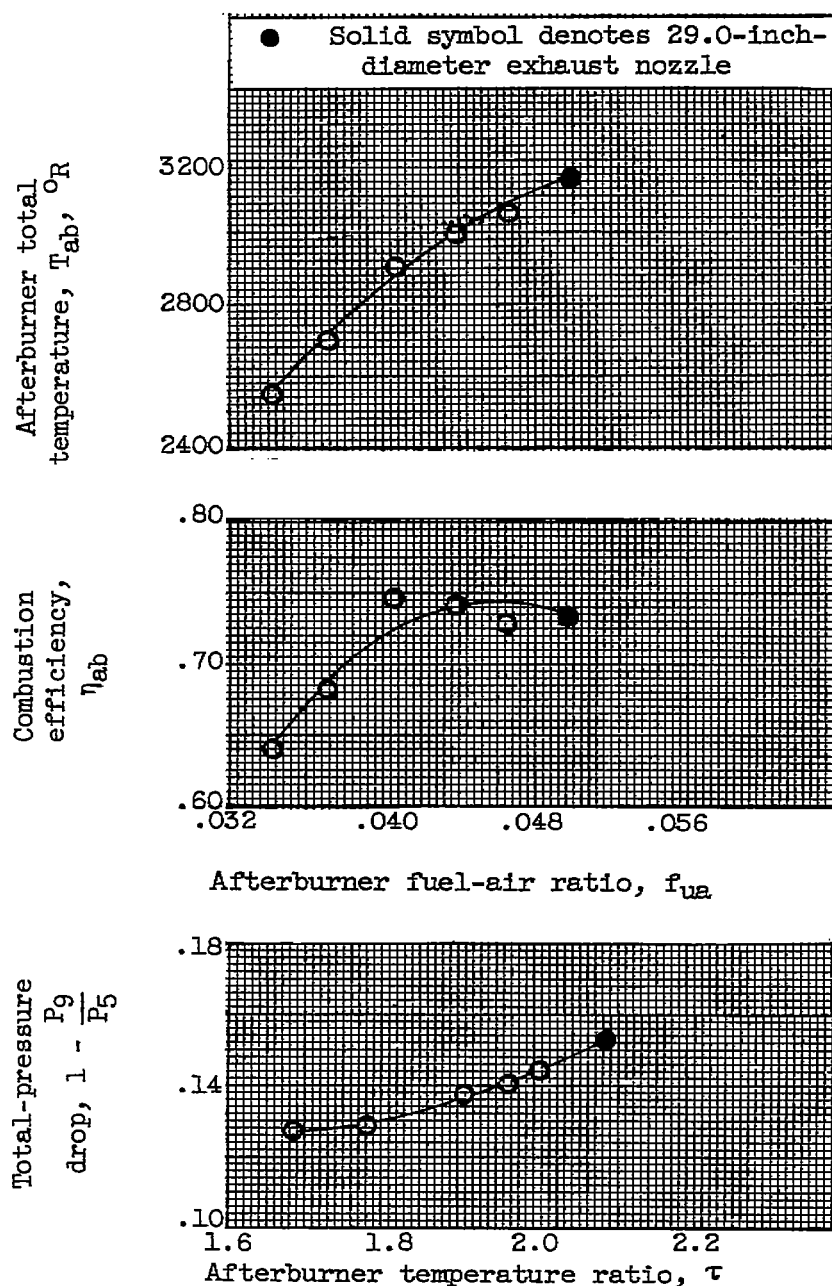


Figure 11. - The variation of afterburner performance parameters with afterburner fuel-air and afterburner temperature ratio at a flight condition of 35,000 feet and a Mach number of 1.16 for the prototype afterburner configuration.

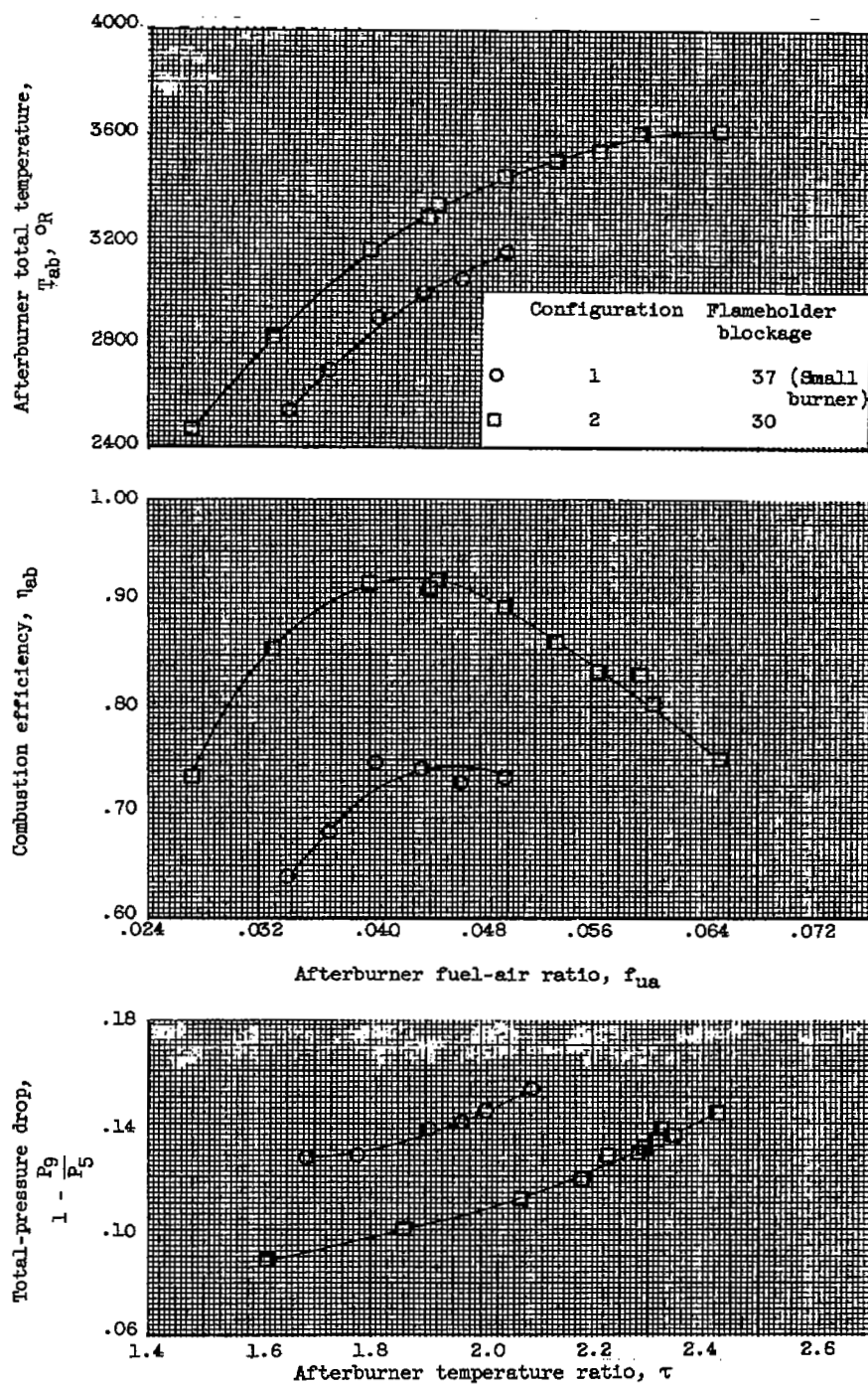


Figure 12. - The variation of afterburner performance parameters with afterburner fuel-air and temperature ratio showing a comparison of configurations 1 and 2. Flight condition, 35,000 feet, Mach number of 1.16.

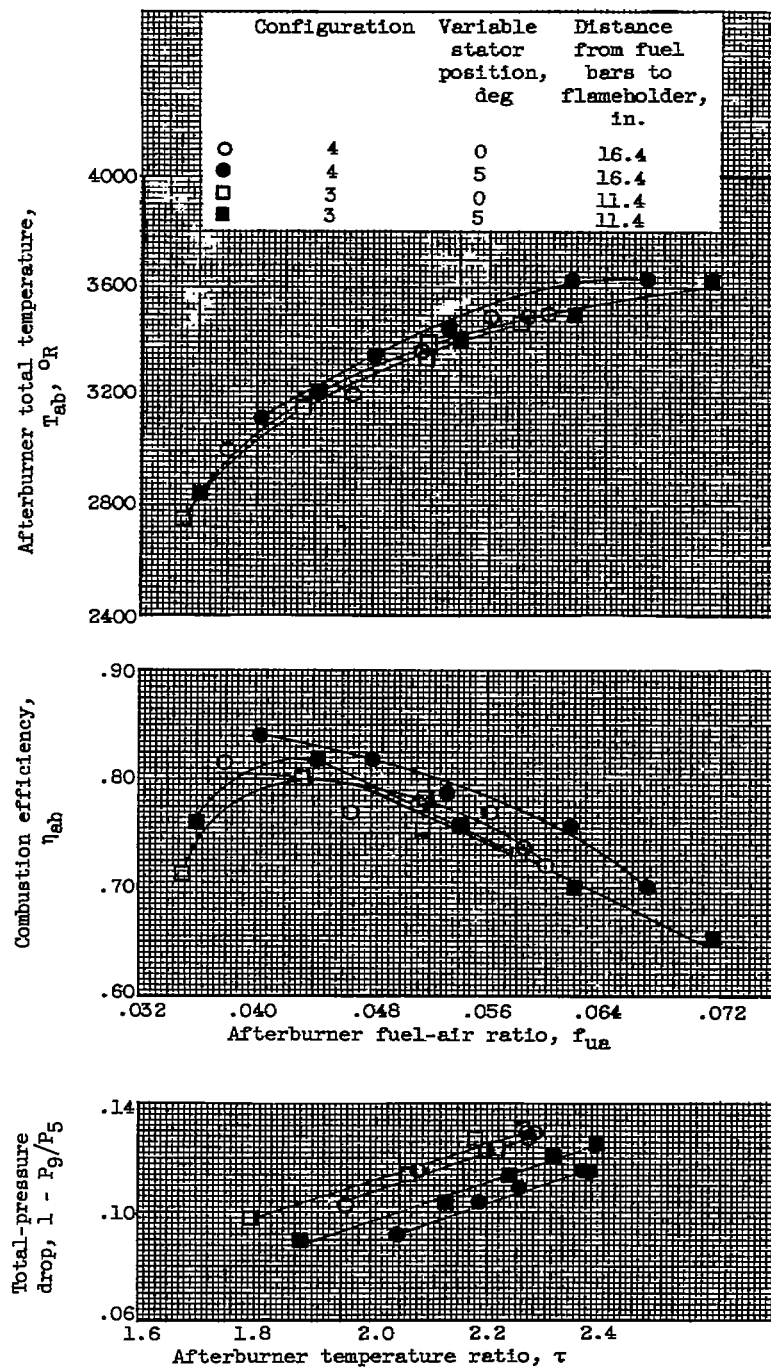


Figure 13. - The effect of variable stator position and flameholder position on the variation of afterburner performance parameters with afterburner fuel-air and temperature ratio. Flight condition, 58,000 feet; Mach number, 2.0; inlet recovery, 85 percent.

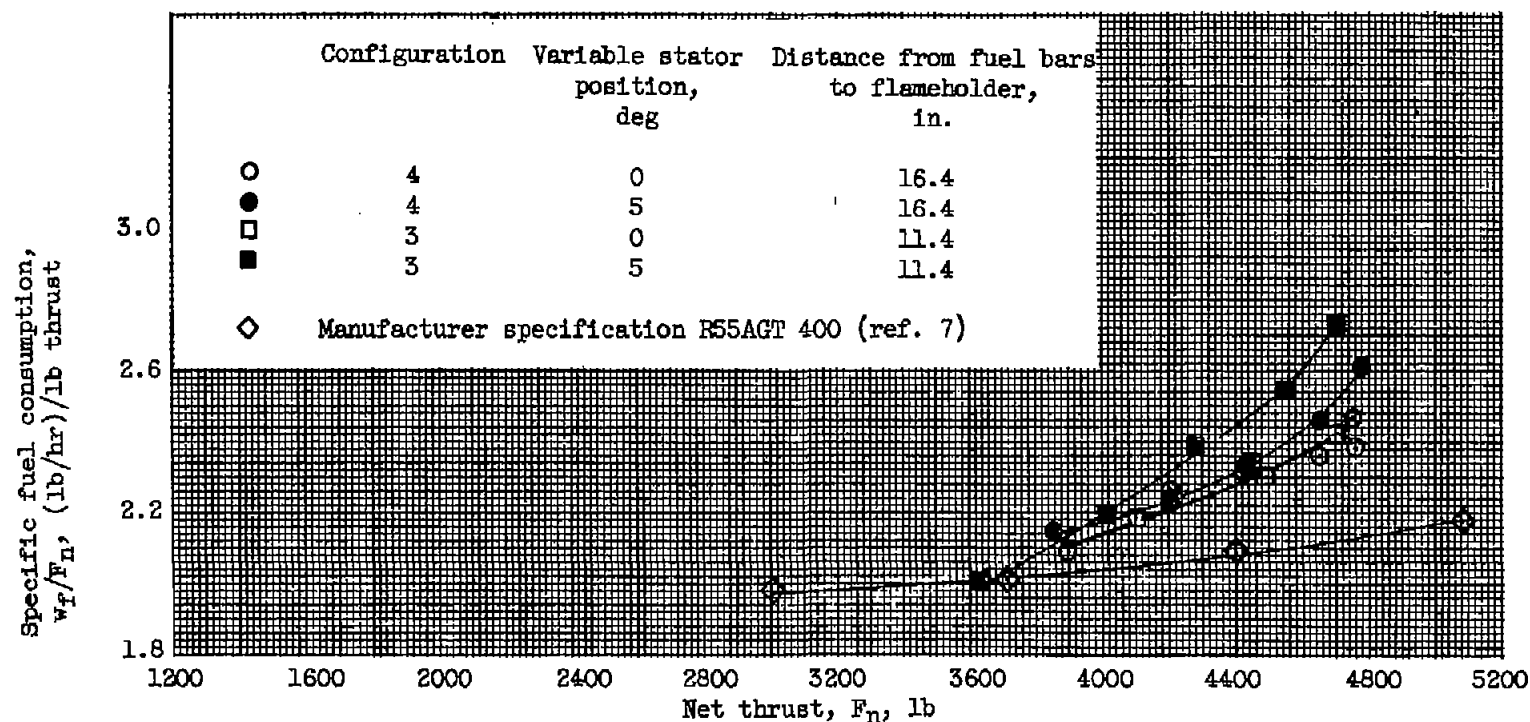
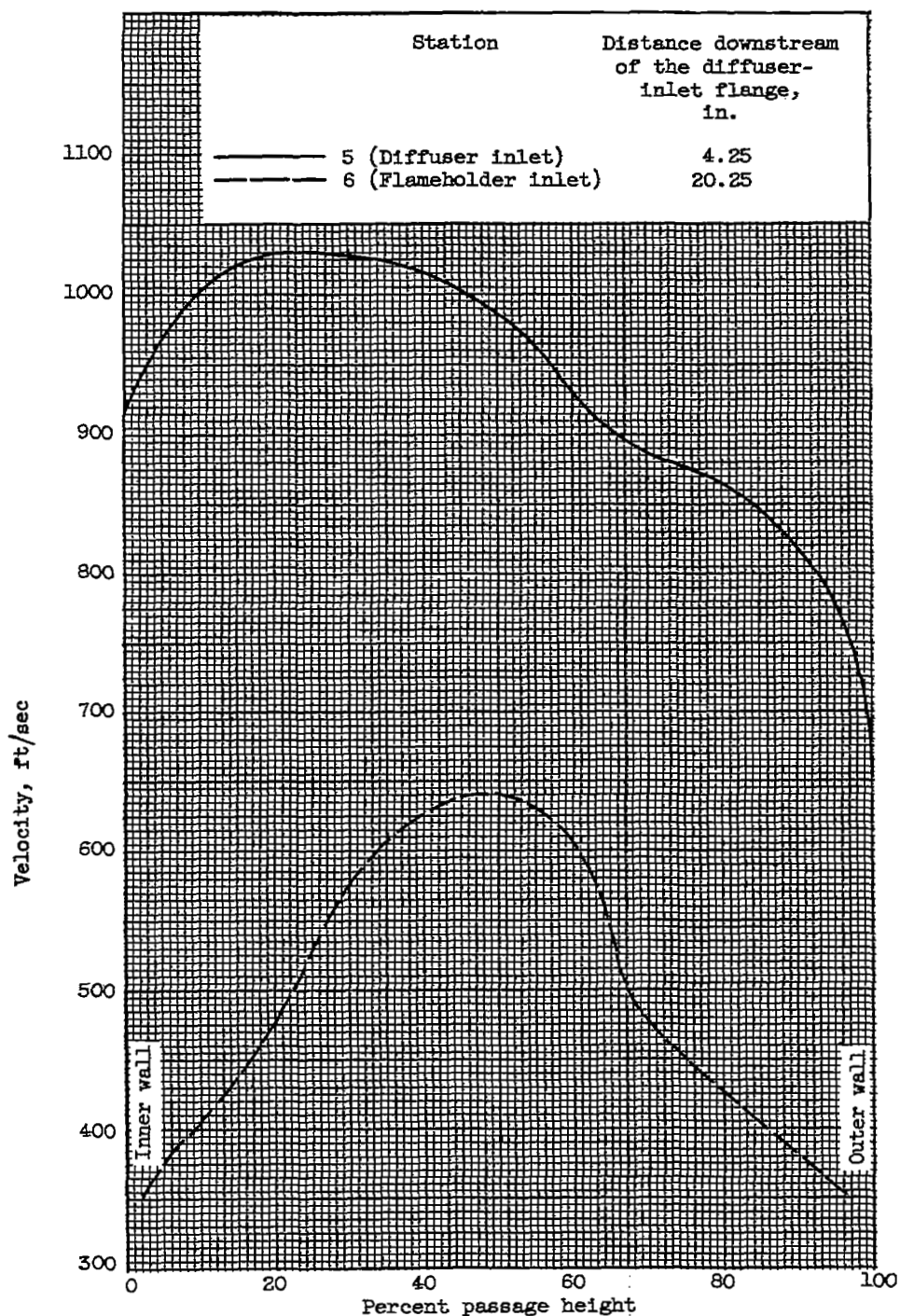
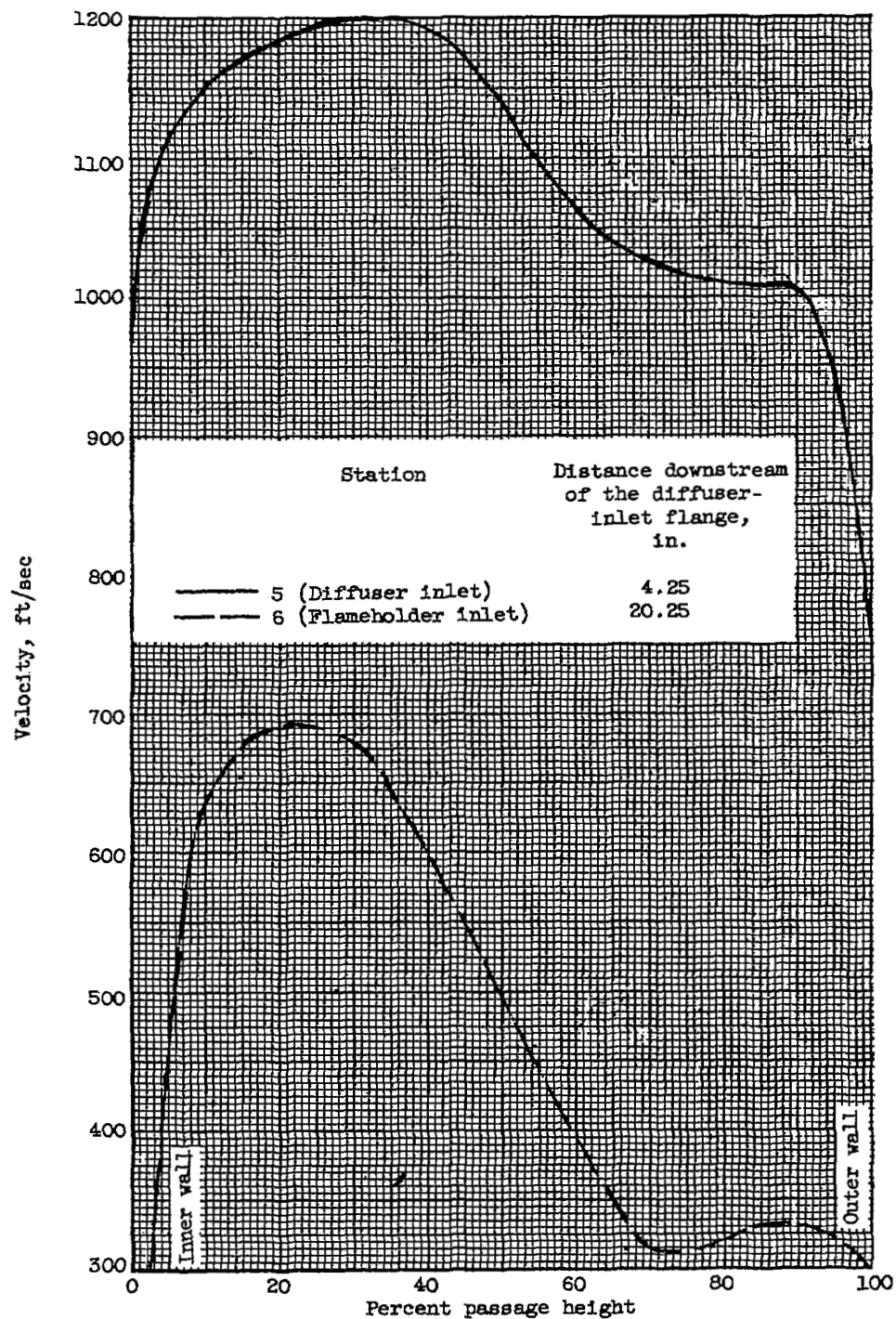


Figure 14. - The variation of specific fuel consumption with net thrust showing a comparison of experimental data with manufacturer specification. Flight condition, 61,400 feet; Mach number, 2.0; ram recovery, 100-percent; secondary flow with typical ejector performance, 7-percent secondary flow (crossplotted from ref. 2, applied to experimental data).



(a) Flight conditions, 35,000 feet; Mach number, 1.16.

Figure 15. - Velocity profiles through the diffuser of the large burner.



(b) Flight condition, 70,000 feet; Mach number, 2.0.

Figure 15. - Concluded. Velocity profiles through the diffuser of the large burner.

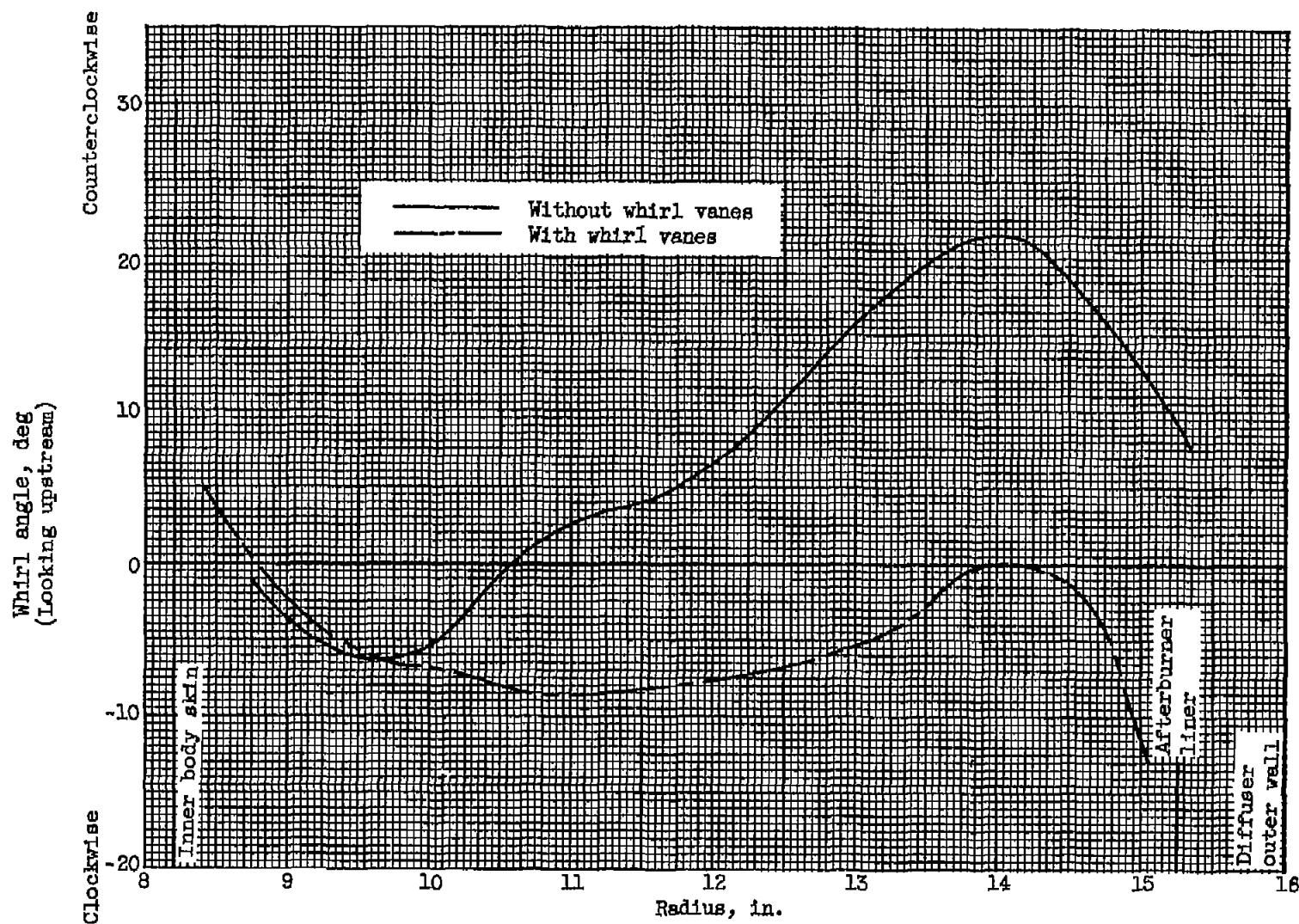


Figure 16. - Whirl profiles existing at fuel bar station (station 5.5) for diffusers with anti-whirl vanes. Flight condition, 35,000 feet; Mach number, 1.16.

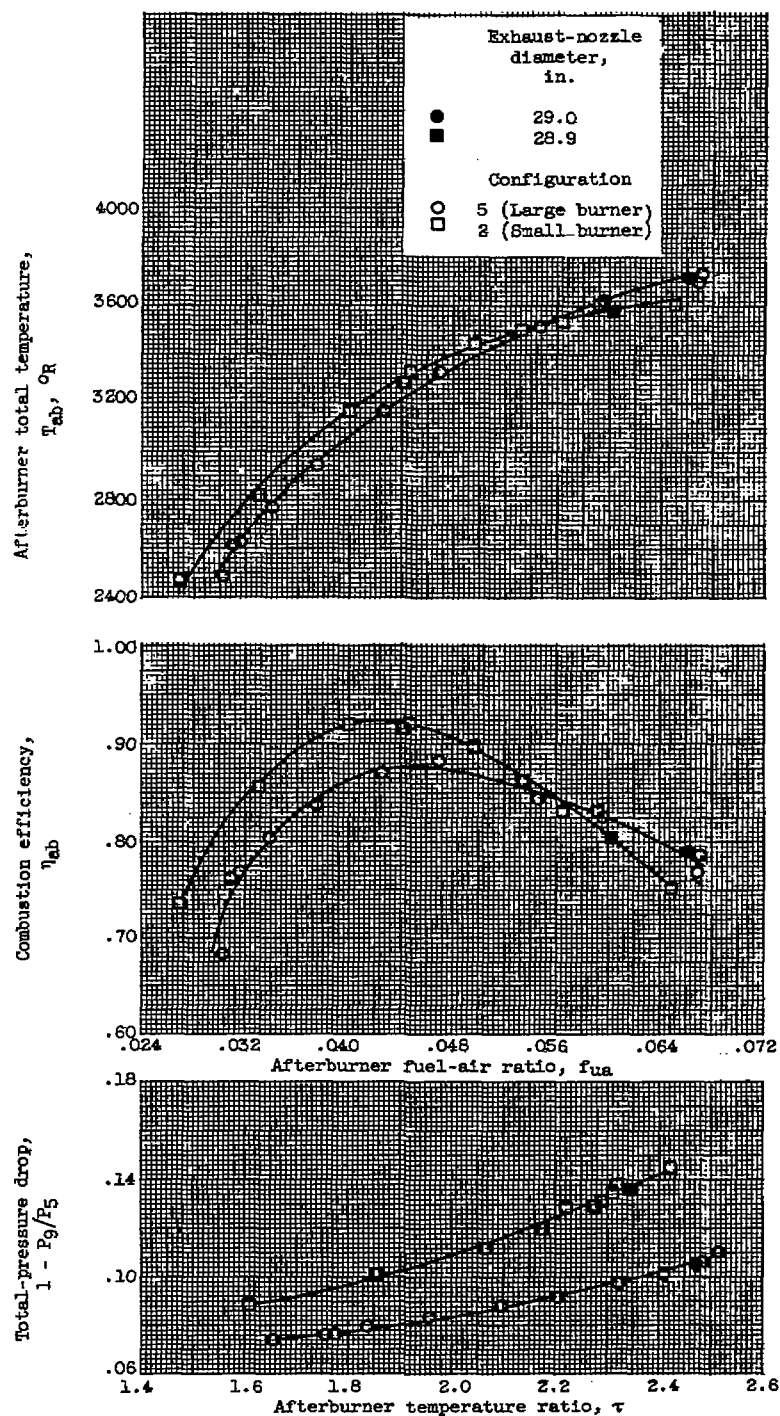


Figure 17. - The variation of afterburner performance parameters for the large burner (small burner, configuration 2, shown for reference). Flight conditions, 35,000 feet; Mach number, 1.16.

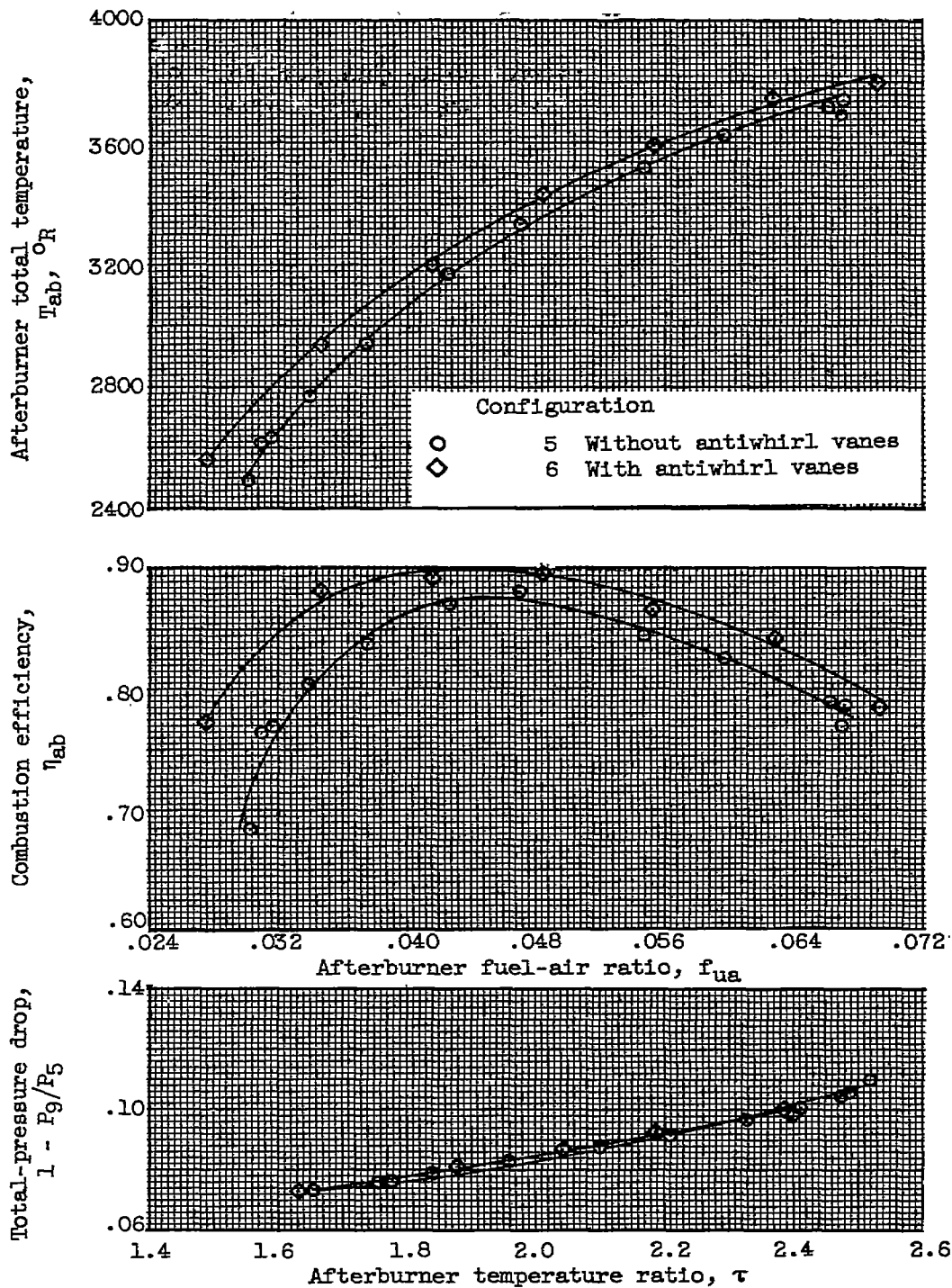


Figure 18. - The effect of installation of antiwhirl vanes on afterburner performance parameters. Flight conditions, 35,000 feet; Mach number, 1.16.

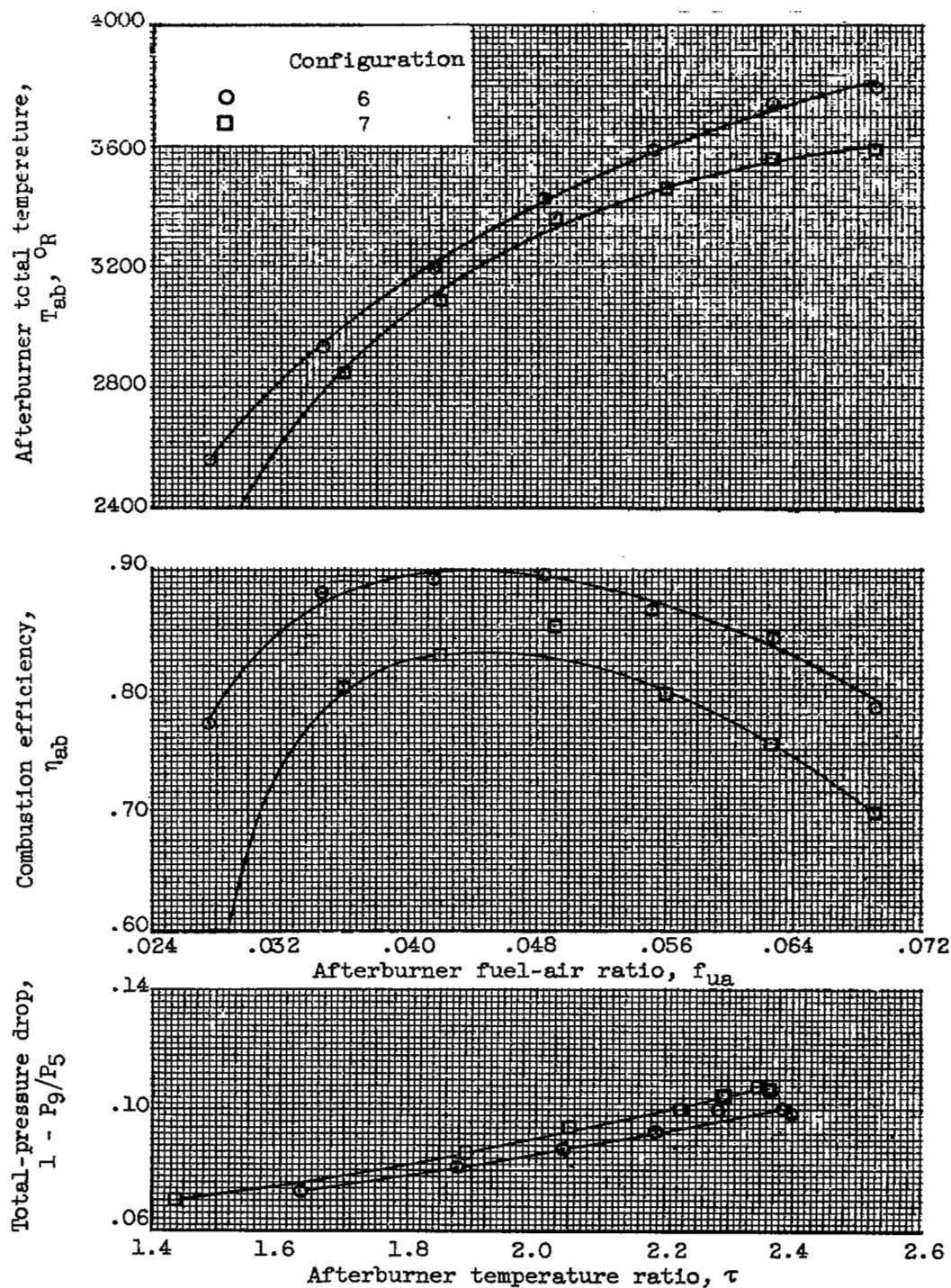


Figure 19. - The effect of fuel distribution on afterburner performance parameters. Flight conditions, 35,000 feet; Mach number, 1.16.

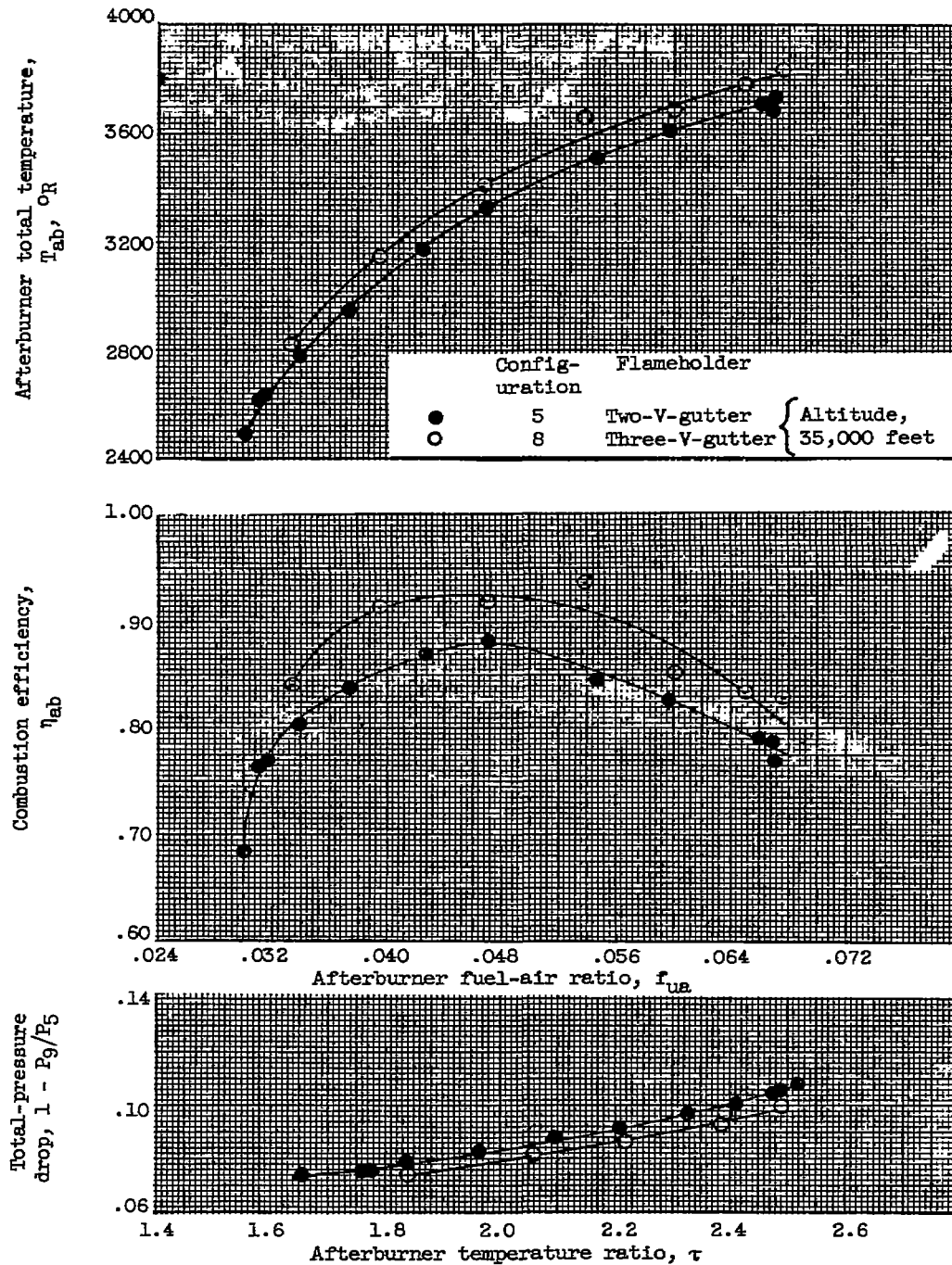
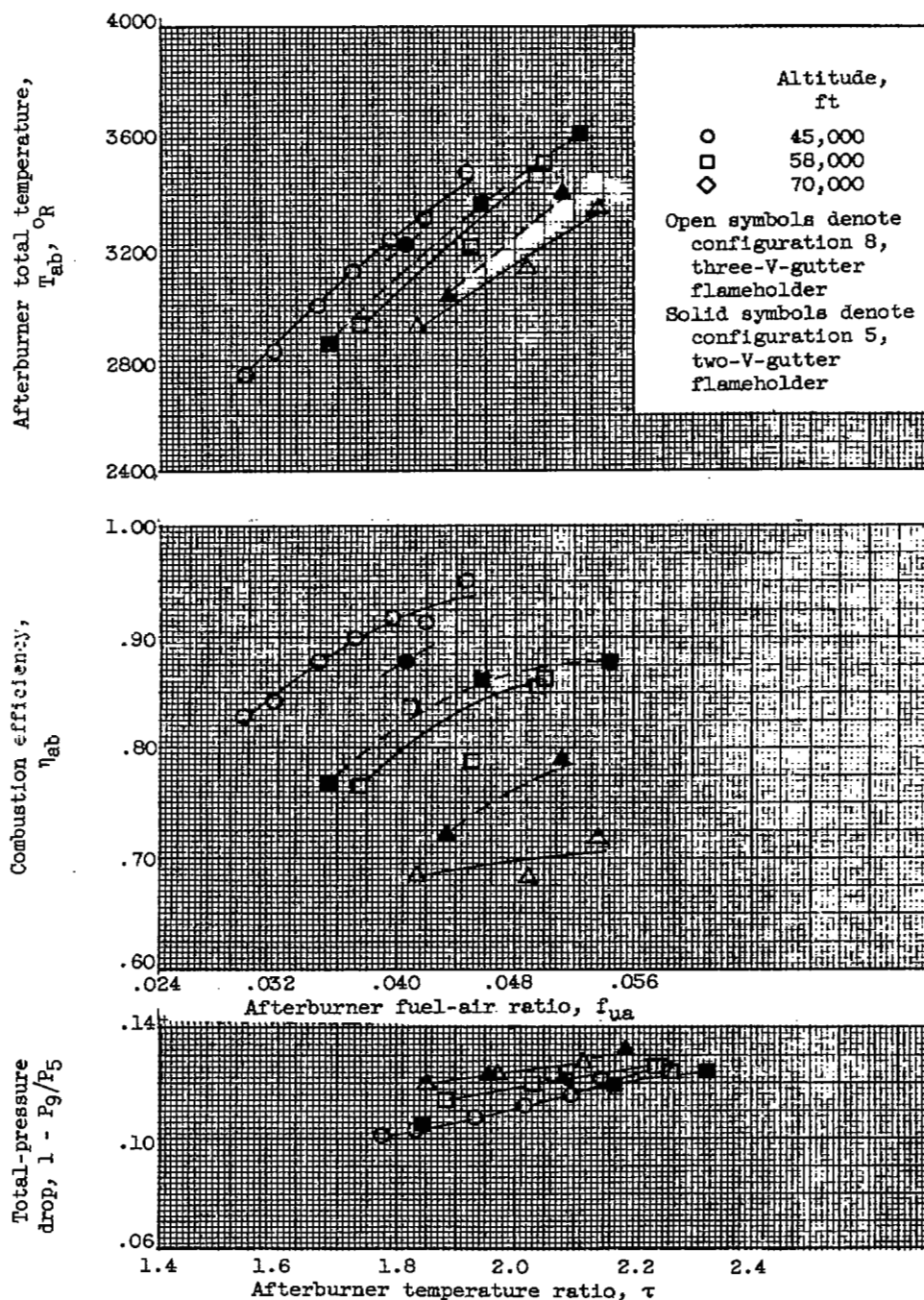


Figure 20. - The effect of flameholder configuration on afterburner performance parameters.



(b) Mach number, 2.0.

Figure 20. - Concluded. The effect of flameholder configuration on afterburner performance parameters.

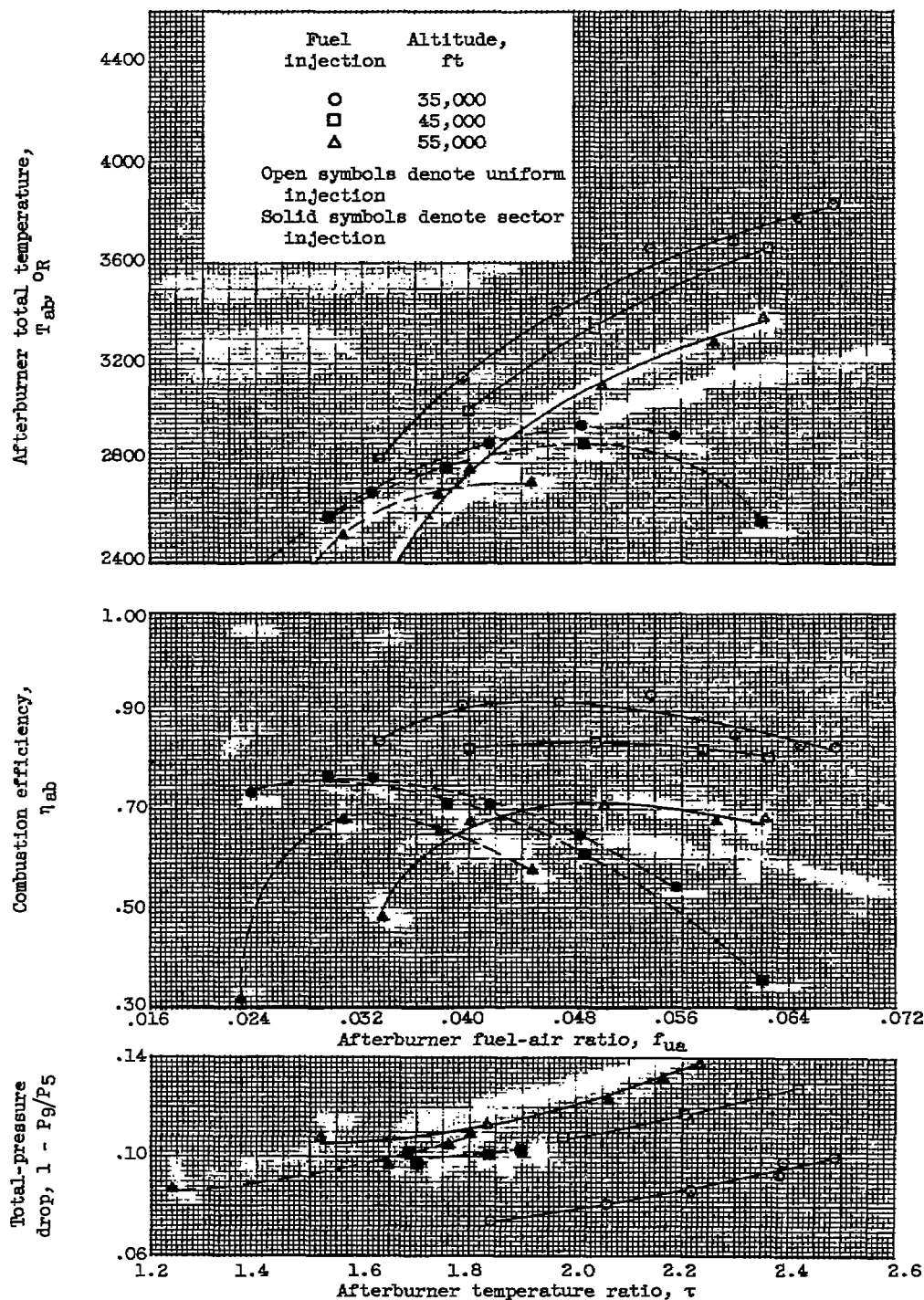


Figure 21. - The effect of sector burning on afterburner performance parameters for configuration 8. Flight Mach number, 1.16.

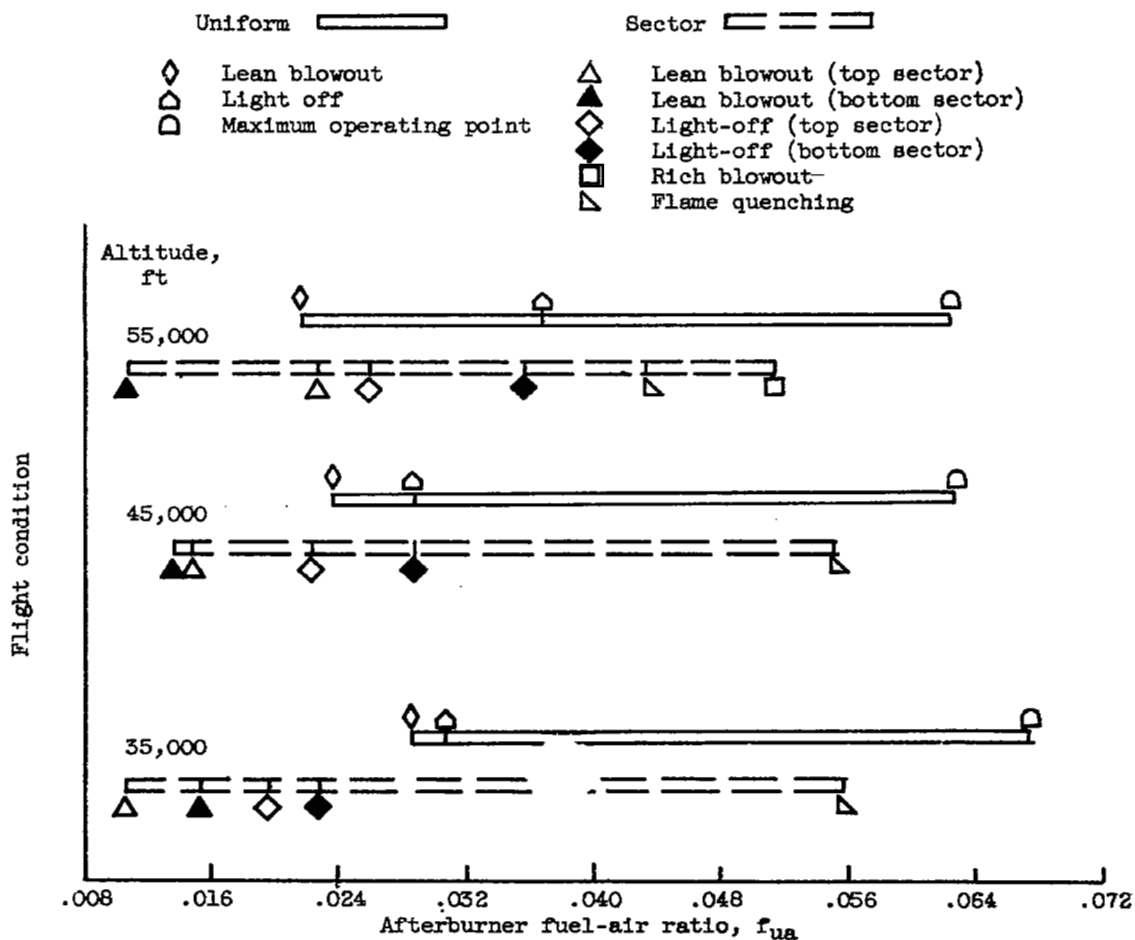
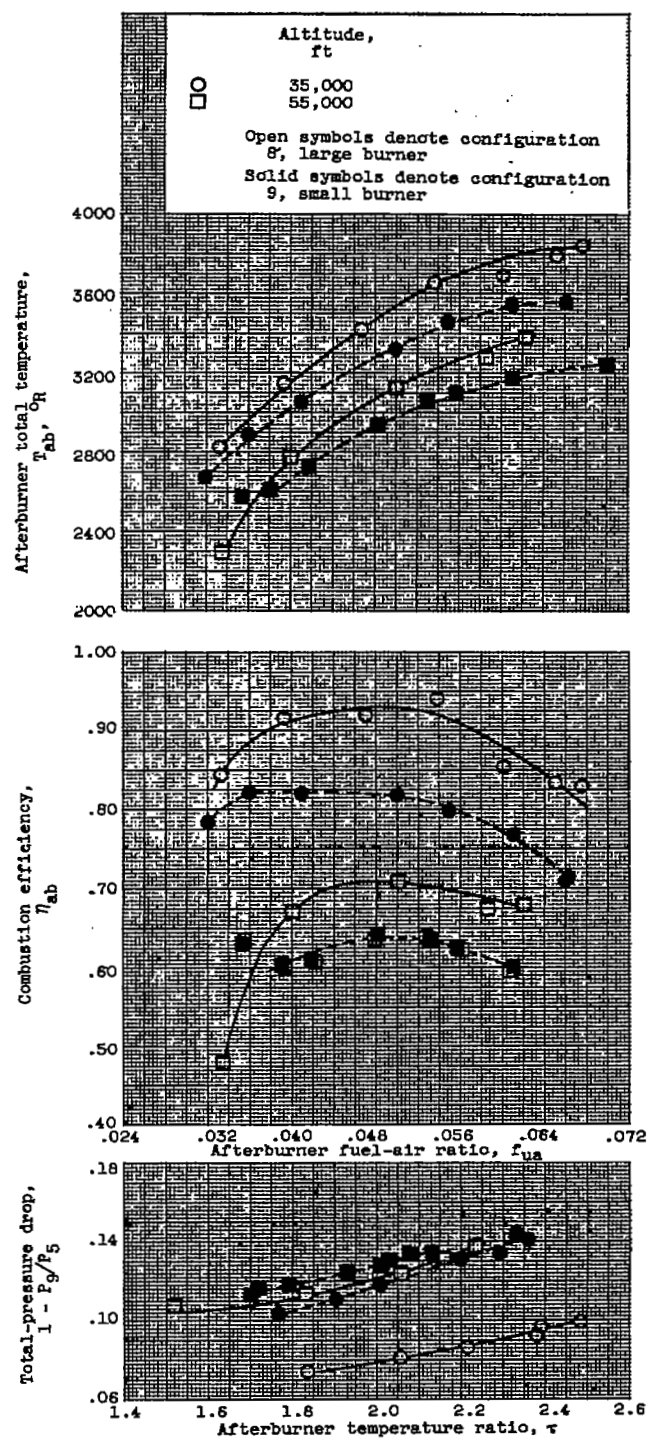
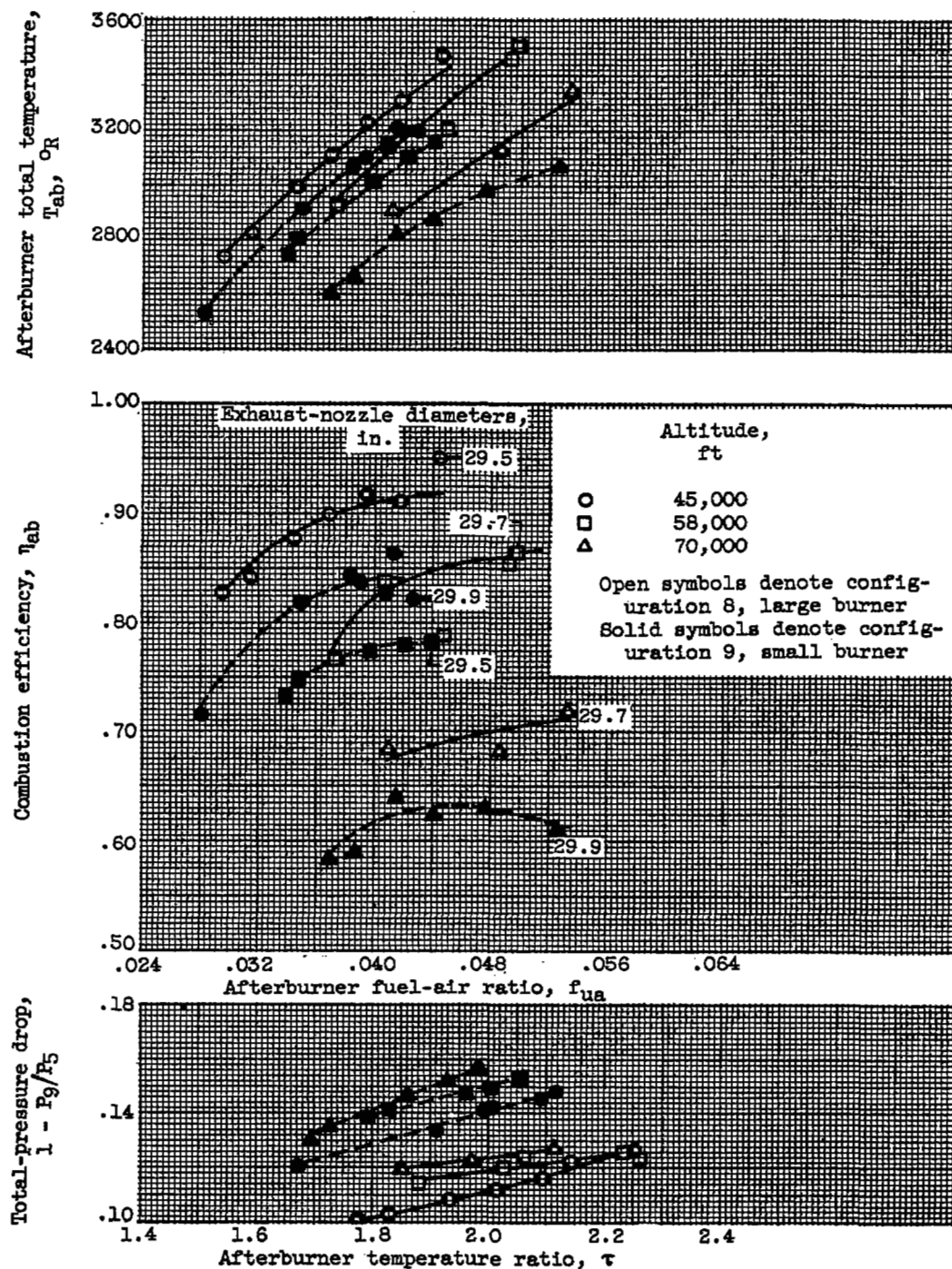


Figure 22. - Afterburner operational characteristics with uniform and sector burning for configuration 8. Flight Mach number, 1.16.



(a) Flight Mach number, 1.16.

Figure 23. - The effect of burner size on afterburner performance parameters.



(b) Flight Mach number, 2.0.

Figure 23. - Concluded. The effect of burner size on afterburner performance parameters.

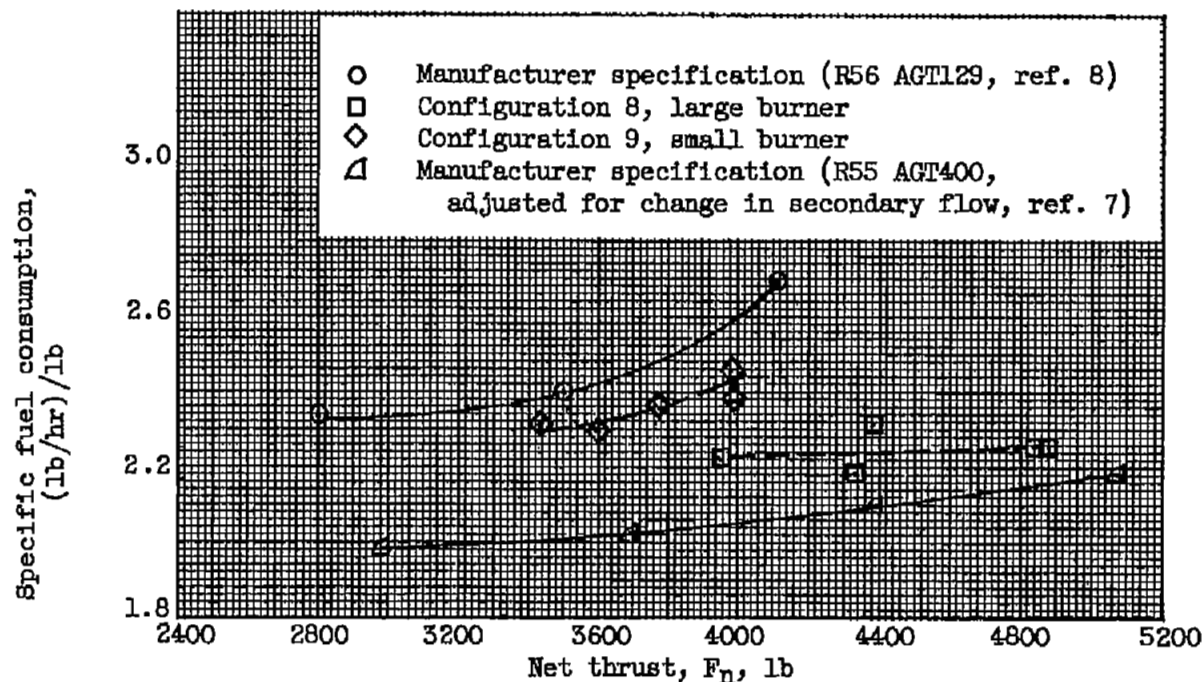


Figure 24. - Variation of specific fuel consumption with net thrust showing comparison of manufacturer specifications with NACA data. Flight condition, 59,400 feet; Mach number, 2.0; inlet recovery, 90 percent. Secondary flow, 8 percent.

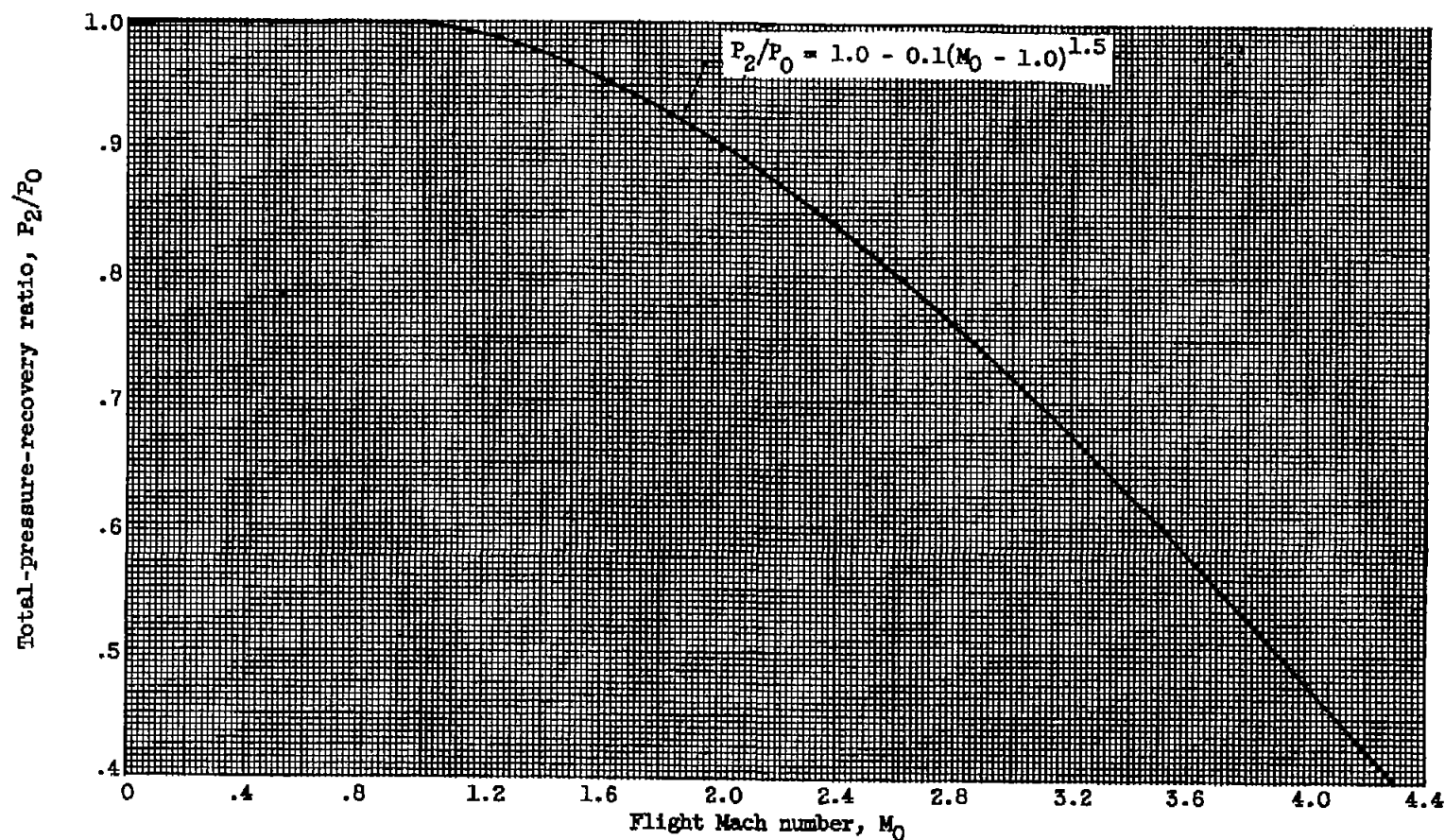


Figure 25. - Standard ram recovery used in reference 8. Standard proposed by the Aircraft Engine Committee of the Aircraft Industries Association.

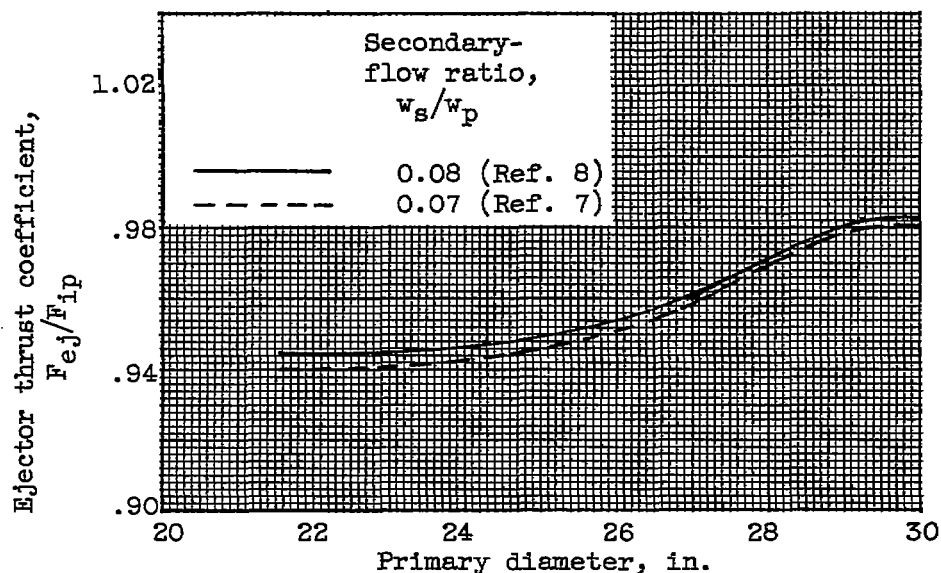
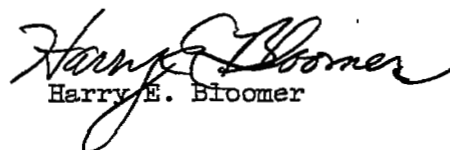
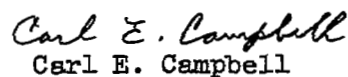


Figure 26. - Estimated ejector thrust coefficient variation with primary diameter (crossplotted from data in refs. 1 and 2). Diameter ratio, 1.25; spacing ratio, 0.71; primary pressure-ratio range, 9.0 to 10.0; primary total-temperature range, 2500° to 3600° R.

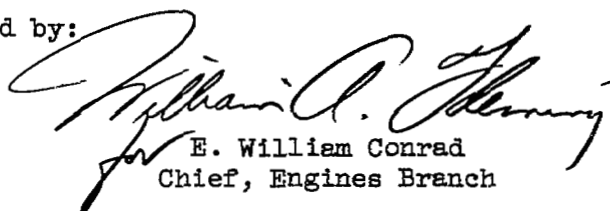
EXPERIMENTAL INVESTIGATION OF SEVERAL AFTERBURNER  
CONFIGURATIONS ON A J79 TURBOJET ENGINE

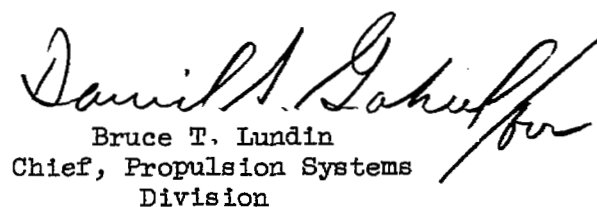
4644

  
Harry E. Bloomer

  
Carl E. Campbell

Approved by:

  
E. William Conrad  
Chief, Engines Branch

  
Bruce T. Lundin  
Chief, Propulsion Systems  
Division

jmp - 9/24/57

NASA Technical Library



3 1176 01435 8783

~~CONFIDENTIAL~~